

**Advanced Exergy Analysis and  
Optimization of Heat Exchanger  
Network under Uncertainty**



**By  
Asad Ayub**

**School of Chemical and Materials Engineering  
National University of Sciences and Technology  
2023**

# **Advanced Exergy Analysis and Optimization of Heat Exchanger Network under Uncertainty**



Name: Asad Ayub

Reg No: 00000361452

**This work is submitted as an M.S. thesis in partial fulfillment of the  
requirement for the degree of**

**M.S. in Process Systems Engineering**

**Supervisor Name: Dr. Iftikhar Ahmad**

**School of Chemical and Materials Engineering (SCME)**

**National University of Sciences and Technology (NUST)**

**H-12 Islamabad, Pakistan**

**December 2023**



### THESIS ACCEPTANCE CERTIFICATE

Certified that final copy of MS thesis written by Mr **Asad Ayub** (Registration No 00000361452), of School of Chemical & Materials Engineering (SCME) has been vetted by undersigned, found complete in all respects as per NUST Statues/Regulations, is free of plagiarism, errors, and mistakes and is accepted as partial fulfillment for award of MS degree. It is further certified that necessary amendments as pointed out by GEC members of the scholar have also been incorporated in the said thesis.

Signature: \_\_\_\_\_

Name of Supervisor: Dr Iftikhar Ahmad

Date: 03-01-2024

Signature (HOD): \_\_\_\_\_

Date: 3/1/24

Signature (Dean/Principal): \_\_\_\_\_

Date: 03.01-2024

**National University of Sciences & Technology (NUST)**  
**MASTER'S THESIS WORK**

Formulation of Guidance and Examination Committee (GEC)

Name: Asad Avub NUST Reg No: 00000361452  
 Department: Department of Chemical Engineering Specialization: Master of Science in Process System Engineering  
 Credit Hour Completed: 24.0 CGPA: 3.75

**Course Work Completed**

S/No:	Code:	Title:	Core/Elective:	CH:	Grade:
1.	PSE-801	Process Systems Theory	Compulsory	3.0	A
2.	PSE-852	Process Modelling and Simulation	Compulsory	3.0	A
3.	TEE-820	Process Intensification	Elective	3.0	B
4.	RM-898	Research Methodology	Additional	2.0	Q
5.	PSE-802	Optimization and Decision Analysis	Compulsory	3.0	A
6.	PSE-823	Advanced Process Dynamics and Control	Compulsory	3.0	A
7.	CSE-801	Computational Fluid Dynamics	Elective	3.0	B+
8.	ENE-809	Waste Water Treatment & Design	Elective	3.0	B+
9.	EME-902	Numerical Methods In Chemical Engineering	Elective	3.0	A

Date 16-Jan-2023

Student's Signature

**Thesis Committee**

- Name: Iftikhar Ahmad (Supervisor)  
Department: Department of Chemical Engineering
- Name: Frum Pervaiz (Cosupervisor)  
Department: Department of Chemical Engineering
- Name: Muhammad Ahsan (Internal)  
Department: Department of Chemical Engineering
- Name: Sher Ahmad (Internal)  
Department: Department of Chemical Engineering

Signature

Signature

Signature

Signature

Date: 16-Jan-2023

Signature of Head of Department:

**APPROVAL**Date: 16-Jan-2023

Signature of Dean/Principal:



Form: TH-04

National University of Sciences & Technology (NUST)

MASTER'S THESIS WORK

We hereby recommend that the dissertation prepared under our supervision by

Regn No & Name: 00000361452 Asad Ayub

Title: Advanced Exergy Analysis and Optimization of a Heat Exchanger Network under Uncertainty.

Presented on: 07 Dec 2023 at: 1430 hrs in SCME

Be accepted in partial fulfillment of the requirements for the award of Master of Science degree in Process System Engineering.

Guidance & Examination Committee Members

Name: Dr Sher Ahmad

Signature: [Signature]

Name: Dr Muhammad Ahsan

Signature: [Signature]

Name: Dr Erum Pervaiz (Co-Supervisor)

Signature: [Signature]

Supervisor's Name: Dr Iftikhar Ahmad

Signature: [Signature]

Dated: 07-12-2024

Head of Department

Date 21/12/24

Dean/Principal

Date 2.1.2024

School of Chemical & Materials Engineering (SCME)

*I have devoted my thesis to my family constant support,  
encouragement, love, and honour.*

## Acknowledgment

All glory and honor belong to "ALLAH," the unequivocal creator of this world, who bestowed upon us the gift of understanding and ignited our inquisitiveness about the entire universe. We extend our most heartfelt greetings to supreme ruler of this world and the hereafter, "Prophet Mohammed (PBUH)," a wellspring of wisdom and blessings for all of humanity, as well as for the Uma.

I would like to express my heartfelt appreciation to my research **supervisor, Dr. Iftikhar Ahmad**. He has consistently offered his firm support, guidance, and warm encouragement, always pointing me in the right direction whenever he felt it was necessary. In addition, I'd like to show my gratitude to my **co-supervisor, Dr. Erum Pervaiz**, for her insightful recommendations and assistance. I am also thankful to **committee members, Dr. Muhammad Ahsan and Dr. Sher Ahmad**, for their invaluable suggestions and guidance.

Furthermore, I extend my thank to **Prof. Dr. Amir Azam Khan**, the Principal of the School of Chemical, for providing a research-oriented platform to effectively utilize my skills in accomplishing this research work.

In conclusion, I want to express my deepest application to my parents for their firm support and constant support throughout my years of study, as well as during the research and writing of this thesis. This achievement would not have been attainable without their presence and guidance.

**Asad Ayub**

# Abstract

In this work, we utilized advanced exergy analysis in conjunction with an integrated framework that combines artificial neural network (ANN) with particle swarm optimization (PSO) and genetic algorithm (GA) to evaluate performance of heat exchangers within a crude oil distillation unit under uncertainty. At the beginning, we constructed an equilibrium-state Aspen model, which subsequently used to conduct both traditional and advanced exergy analyses. This exergy analysis enabled us to quantify exergy efficiency and the level of irreversibility within the heat exchanger network (HEN). Subsequently, we calculated four components of irreversibility—endogenous, exogenous, avoidable, and unavoidable—for the equipment exhibiting significant incompetence with advanced exergy analyses. The operational model was subsequently converted into a dynamic configuration by introducing  $\pm 10\%$  fluctuation into system variables, such as temperature, and mass flow rate, resulting in the creation of a dataset comprising 600 samples. Five ANN models were developed using this dataset, each designed to predict various aspects, including overall exergy efficiency, exergy destruction, modified exergy efficiency, unavoidable exergy destruction and avoidable exergy destruction. ANN model served as a substitute within the PSO and GA environment to optimize HEN under uncertain condition. The optimized operational parameters obtained within the PSO and GA methods were further validated by feeding them into Aspen model for validation through cross-referencing. The exergy analysis revealed that HEN had 66.16% exergy efficiency, and the exergy destruction was 5403.166 kW. Advanced exergy analysis further revealed that avoidable exergy destruction amounted to 1,759.80 kW, while unavoidable exergy destruction stood at 3,643.35 kW. Seven heat exchangers, displaying the highest exergy destruction rates, were identified as priority candidates for intervention due to their significant impact on the network. The effectiveness of both the GA and PSO optimization methods exhibited similar results, and they notably enhanced the exergy performance of the facility when correlate to the standalone Aspen model of the process.

**Keywords:** Heat Exchanger Network, CDU, Advanced Exergy Analysis, Uncertainty, Artificial Neural Network, Genetic Algorithm, Particle Swarm Optimization, Exergy Efficiency; Machine learning



# Table of Contents

List of Figures .....	vi
List of Tables.....	vii
Nomenclature.....	viii
Chapter 1 Introduction .....	1
1.1 Background .....	1
1.2 Objectives.....	3
1.3 Thesis outline .....	3
Chapter 2 Literature Review .....	4
2.1 Literature review .....	4
Chapter 3 Process Description and Methodology.....	8
3.1 Process description.....	8
3.2 Thermodynamic properties .....	10
3.3 Conventional exergy analysis.....	11
3.4 Advanced exergy analysis.....	12
3.4.1 Splitting exergy destruction .....	12
3.4.2 Avoidable and unavoidable exergy destruction .....	13
3.4.3 Endogenous and exogenous exergy destruction .....	14
3.5 Artificial neural network .....	15
3.5.1 The Levenberg-Marquardt method .....	17
3.6 Genetic algorithm.....	17
3.6.1 Genetic operators .....	18
3.7 Particle swarm optimization.....	21
3.8 Surrogate model .....	23
3.9 Methodology .....	23
3.9.1 Phase-I: Steady-state conventional and advanced exergy analysis.....	23

3.9.2	Phase-II: Data generation.....	25
3.9.3	Phase-III: ANN modelling .....	26
3.9.4	Phase-IV: Optimization.....	27
Chapter 4 Results and Discussion.....		29
4.1	Steady-state exergy analysis.....	30
4.2	Steady-state advanced exergy analysis .....	31
4.3	Data based modelling .....	35
4.3.1	ANNs development.....	35
4.3.2	Exergy efficiency .....	35
4.3.3	Exergy destruction .....	36
4.3.4	Avoidable exergy destruction.....	37
4.3.5	Unavoidable exergy destruction.....	37
4.3.6	Modified exergy efficiency .....	38
4.4	Optimization.....	39
4.4.1	Optimization of exergy efficiency of heat exchanger network:.....	39
Conclusion.....		42
Reference.....		43

# List of Figures

<b>Figure 1:</b> Forecast of industrial energy demand by 2040 .....	1
<b>Figure 2:</b> Scheme of Preheat Train of the Crude Distillation Unit .....	9
<b>Figure 3:</b> Exergy destruction splitting of a component k.....	13
<b>Figure 4:</b> Line obtained by graphical method for endogenous exergy destruction) .....	15
<b>Figure 5:</b> General representation of weights and biases for ANN .....	16
<b>Figure 6:</b> General ANN architecture .....	16
<b>Figure 7:</b> Schematic representation of Genetic Algorithm .....	18
<b>Figure 8:</b> Roulette wheel selection for the population .....	19
<b>Figure 9:</b> Tournament selection in GA.....	20
<b>Figure 10:</b> Single point crossover .....	20
<b>Figure 11:</b> Double point crossover .....	21
<b>Figure 12:</b> Uniform points crossover .....	21
<b>Figure 13:</b> Workflow of particle swarm optimization.....	22
<b>Figure 14:</b> Methodology in this research .....	25
<b>Figure 15:</b> Exergy Destruction Percentage .....	31
<b>Figure 16:</b> Avoidable and Unavoidable Exergy Destruction .....	32
<b>Figure 17:</b> Avoidable Exergy Destruction of Heat Exchangers.....	33
<b>Figure 18:</b> Effect of Avoidable Exergy Destruction on Exergy Efficiency.....	33
<b>Figure 19:</b> Endogenous and Exogenous Exergy Destruction .....	34
<b>Figure 20:</b> Predicted vs actual exergy efficiency of Heat Exchanger Network .....	36
<b>Figure 21:</b> Predicted vs actual exergy destruction of heat exchanger network.....	36
<b>Figure 22:</b> Predicted vs actual avoidable exergy destruction of heat exchanger network .....	37
<b>Figure 23:</b> Predicted vs actual unavoidable exergy destruction of heat exchanger network ..	38
<b>Figure 24:</b> Predicted vs actual modified exergy efficiency of heat exchanger network .....	38

## List of Tables

<b>Table 1:</b> Chromosomes representation of general GA .....	18
<b>Table 2:</b> Real, Unavoidable and Theoretical condition for each Heat Exchanger .....	24
<b>Table 3:</b> Some Data Samples after uncertainty .....	26
<b>Table 4:</b> Characteristics for each state within the preheat train .....	29
<b>Table 5:</b> Exergy Destruction, Exergy Efficiency, and Exergy Destruction Ratio .....	30
<b>Table 6:</b> Avoidable and Unavoidable Exergy Destruction .....	32
<b>Table 7:</b> Endogenous and Exogenous Exergy Destruction .....	34
<b>Table 8:</b> Genetic algorithm parameters used to optimize the exergy efficiency .....	39
<b>Table 9:</b> PSO parameters used to optimize the exergy efficiency .....	39
<b>Table 10:</b> Comparison of SA, GA, and PSO exergy efficiency of heat exchanger network...	40
<b>Table 11:</b> GA and PSO performance validation of heat exchanger network.....	40

## Nomenclature

HEN	Heat exchanger networks
ANN	Artificial Neural Network
BPD	Barral Per Day
GHG	Greenhouse Gas Emissions
GA	Genetic algorithm
PSO	Particle swarm optimization
CDU	Crude Oil Distillation Unit
TAC	Total Annual Consumption
ABC	Artificial Bee Colony
CCPC	Combine Cycle Power Plant
DB	Duct Burners
NSGA-II	Non-dominated Sort Genetic Algorithm-II
WSH-MES	Wind-Solar-Hydrogen Multi-Energy Supply
SR	Straight Run
HVGO	Heavy Vacuum Gas Oil
MVGO	Medium Vacuum Gas Oil
AGO	Atmospheric Gas Oil
HDiesel	Heavy Diesel
VR	Vacuum Residue
PHT	Preheat Train
SUS	Stochastic Universal Sampling
ROM	Reduce Order Model
B	Bais

$E_D$	Exergy Destruction
$E_F$	Fuel Exergy
$E_P$	Product Exergy
$E_{in}$	Exergy in
$E_{out}$	Exergy out
$E_{ph}$	Physical Exergy
$E_{KN}$	Kinetic Exergy
$E_{PT}$	Potential Exergy
$E_{CH}$	Chemical Exergy
$E_{AV}$	Avoidable Exergy
$E_{UN}$	Unavoidable Exergy
$E_{EN}$	Endogenous Exergy
$E_{EX}$	Exogenous Exergy

# Chapter 1

## Introduction

### 1.1 Background

The exhaustion of fossil fuel reserves, environmental concerns, increasing industrialization, and the corresponding global rise in energy demand and utilization have prompted the practical and sustainable use of energy [1, 2]. Energy is vital in today's modern world, and the petrochemical sector is its cornerstone. The primary products of the petrochemical industry are consumer chemicals, specialized chemicals, and basic chemicals. They encompass a wide range of products across sectors including energy, buildings, transportation, pharmaceutical, electronics and telecommunication. As the largest sector with energy-intensive production processes, it contributed approximately 37% of global energy consumption and accounted for around 13% of worldwide greenhouse gas emissions (GHG). Moreover, a 40% increase in consumption is expected by the year 2040, as presented in Figure 1.

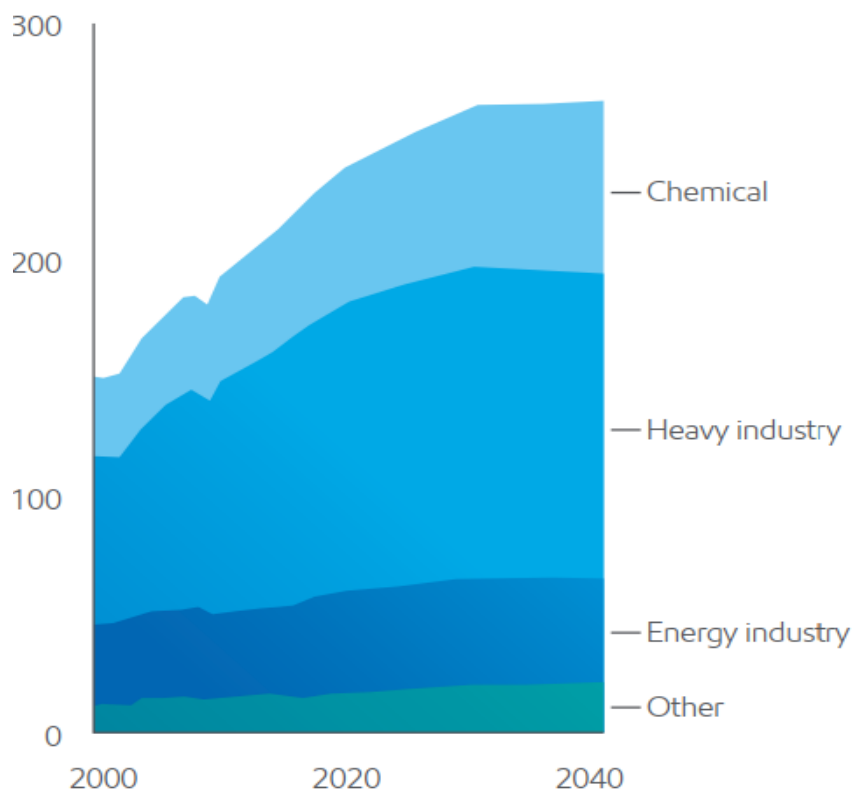


**Figure 1:** Forecast of industrial energy demand by 2040 [3]

Within the spectrum of petrochemical industries, the petroleum refinery ranks among the most energy-consuming, accounting for 33% of total industrial energy consumption. Petroleum refineries consume energy amounting to 30349,01(104 GJ) due to the substantial heat required for oil fractionation [4, 5]. Due to this high energy consumption, energy minimization of refining processes is essential.

To minimize the total energy usage in refining operations heat exchanger networks (HEN) are used [6]. These units are employed to integrate cold and hot streams in the process, harnessing the residual heat from hot streams. By employing HEN heat provided by an external source is reduced and overall process efficiency is increase. However, there are some elements such as fouling, aging, and oil components that influence the execution of heat exchangers. Due to the lower efficiency of heat exchangers due to these factors, energy requirement in the process increases, and consequently, the overall efficiency of the process decreases [7-9].

Conventionally, pinch and exergy analyses are utilized to improve the effectiveness of HEN. Pinch analysis is grounded in the first law of thermodynamics. However, it primarily identifies potential heat recovery and the lowest energy demand or highest energy retrieval from the processes. In contrast, exergy analysis combines the fundamental principles of thermodynamics to discern the genuine thermodynamic enhancement possibilities within the system [10]. However mutual dependencies among the components of the system cannot be assessed by the traditional exergy analysis and due to this its result could lead to some misinterpretation [11]. A recently developed technique, the advanced exergy analysis method can assess the interconnections among the components of the system by dividing the exergy destruction of each element into intrinsic and extrinsic components. Further subdividing the exergy destruction into preventable and inevitable segments provides a more realistic assessment of the potential for improvement [12].

Together conventional and advanced exergy analysis are potential tools that can accurately identify the location, magnitude, cause of exergy destruction in the operation. Furthermore, it can analyse the interconnections among system components and offer a practical evaluation of potential to enhance the system components by dividing the exergy destruction. Enhancing processes through advanced exergy analysis promotes the efficient use of natural reserves and contributes to environmentally friendly practices.

The use of advanced exergy analysis is broadly studied to optimize the performance and for the design of various industrial processes like chemical [13], milk [14], cement [15], coal



gasification [16], and petrochemical [17]. However, the advanced exergy analysis method encounters challenges in handling uncertainty in process conditions due to the difficulties of modelling undertakings and the extensive computational time required. This research aims to build a computational model that can efficiently be employed during the chemical industries' designing or operational stage to deal with uncertainty. This tool should be rigorous enough to handle the complicated calculations required for advanced exergy analysis while still being adaptable enough to be modified as needed.

## **1.2 Objectives**

The following are the objectives of the thesis,

- Advanced exergy analysis of the heat exchanger network.
- Development of a machine learning model to estimate the exergy efficiency of the heat exchanger network under uncertainty.
- Utilize a machine learning model as a surrogate within GA and PSO framework to optimize the exergy efficiency of the heat exchanger network beneath uncertain conditions.

## **1.3 Thesis outline**

The thesis arrangement is as follows. Chapter 1 provides an overview of the background and outline the research objectives. Further a detailed literature review is discussed in chapter 2. Process description and flowsheet is presented in Chapter 3 along with methodology and theoretical background of Advanced Exergy Analysis, ANN, GA and PSO. Results are discussed in Chapter 4.

# Chapter 2

## Literature Review

### 2.1 Literature review

Researchers have been focusing on streamlining petroleum refining processes to reduce energy consumption and optimize overall system performance. HEN play a key role in reducing overall energy consumption during refining processes. Traditionally, pinch and exergy analysis have been employed to enhance HEN efficiency. Pinch analysis focuses on identifying potential heat recovery and minimum energy requirements within the processes, while exergy analysis unveils the true thermodynamic improvement potential within the system. However, conventional approaches have their limitations when it comes to assessing mutual interdependencies among system components, which can sometimes result in misinterpretation. A recently innovated method, advanced exergy analysis, overcomes this limitation by evaluating the mutual interdependencies among system components. This is achieved by dissecting the exergy destruction within every constituent into exogenous, endogenous, avoidable, and unavoidable segments. This comprehensive breakdown offers a more realistic assessment of the system's potential for enhancement.

Numerous studies, primarily grounded on the first principle of thermodynamics have been conducted to enhance the effectiveness of HEN. For example, BH Li et al [18]. employed a retrofit method centered on pinch analysis to minimize utility consumption in HEN by adopting the new minimum temperature approach, involving a minor capital investment. For demonstration of the effectiveness of this approach, they retrofit an industrial case, specifically a crude oil preheat train. This application of this approach led to an increase in energy savings ranging from 45% to 75%, surpassing previously reported values. Liang et al [19]. proposed an alternative HEN design by using the pinch and retrofit analysis which will save energy up to 7595 kW. The decrease in hot and cold utility consumption is 14.6% and 22.3% respectively. Ulyev et al [20]. also did retrofitting through pinch analysis which reduced the energy utilization up to 6.4MW and led to a decrease of 35.5% and 51.9% in hot and utility demand respectively. IH Alhajri et al [21]. used pinch analysis for the optimization of crude oil distillation operations by retrofitting an existing HEN. By using this approach about 10.4 MW of energy can be conserved in comparison to the current process, resulting in annual running

cost reductions of around MM2 and achieving a return on investment period of under twelve months. MA Gadalla et al [22]. Introduce a novel graphical method, grounded in pinch analysis, this study explores heat recovery systems, particularly their applicability to HEN retrofit. The innovative graphical representation simplifies the identification of key elements, including exchangers situated throughout the pinch point, the network pinch, matching pinches, and the inefficient distribution of fuel utilization. This graphical tool can also aid in pinpointing potential enhancements to boost energy efficiency. Application of this approach to a specific case study resulting in impressive reserves of around 17% in energy consumption and fuel usage. S Mrayed et al [23]. proposed a retrofitting design of the HEN of an existing CDU by using the pinch analysis for the improvement of HEN thermal efficiency. The maximum cooling and heating utility of around 67.5 MW can potentially be reclaimed, in contrast to the current utility demand of 148.6 MW. Babaqi et al [24]. reduced the utility demand by 16.20% by adding more heat exchanger surface to enhance energy recovery efficiency, achieved through the application of pinch analysis in conjunction with PSO.

Numerous studies employing exergy analysis on HEN efficiency improvement have been documented in the existing literature. Like, C Yan et al [25]. proposed an optimization framework for the retrofitting of CDU system grounded on the exergy analysis. The improved manner saw a notable increase in exergy efficiency, rising from 28.9% to 41.4%. Simultaneously, the total annual consumption (TAC) witnessed a significant reduction of 28.7%. These improvements were achieved while maintaining the same product features and flow rates. M Mehdizadeh et al [26]. perform the exergy analysis on estimating the distribution of irreversibility and the exergy destruction in a complex natural gas refinery's HEN. The study findings revealed that the predominated sources of exergy destruction within the entire HEN of the plant stems from irreversibility due to heat transfer, contributing to approximately 84.2% of the total. Furthermore, the overall exergetic efficiency was determined to be 63.34%, indicating substantial room for improvement within the system. In [27]. authors established and optimized the heat exchanger network by employing the combined approach of exergy analysis and pinch method.

Advanced exergy analysis, which incorporating both first and second principle of thermodynamics, is gaining considerable attention among researchers due to its capacity to evaluate the mutual interdependencies and enhancement potential of system components. Various research has been carried out on the assessment of HEN using advanced exergy analysis. For instance, M Mehdizadeh et al [28]. assess the unavoidable and avoidable exergy

destructions within the HENs of a complex natural gas refinery by using advanced exergy analysis. The objective of this study was only to improve the avoidable part of exergy destruction. From the results, it seems that exergy efficiency of the HEN in the process is 62.8% which could be improved up to 84.2%, and approximately 59% of the overall irreversibility within the system is preventable and thus, can be eradicated. F B" uhler et al [14]. perform an evaluation of the milk powder production facility. This analysis encompasses the utilization of various methods like energy, exergy, and advanced exergy methods. The energy assessment has determined that the capacity for integrating heat inside the facility is limited. The exergy analysis has identified that the gas burner and spray dryer are the major sources of exergy destruction, while the heaters exhibit low exergy efficiencies. The advanced exergy analysis has further revealed that the evaporators contribute significantly to avoidable exergy destruction within the facility. J Fajardo et al [29]. apply both conventional and advanced exergy analysis to the HEN of CDU. The aim was to identify the most economical periods for the performing maintenance tasks on the exchangers. The findings of the study have shown that approximately 63% of exergy destruction within the HEN can be prevented. Additionally, five heat exchangers were identified as critical, as they exhibited the highest rates of exergy destruction, making them a priority for maintenance activities.

As the industry moves towards AI-driven smart manufacturing, also known as Industry 4.0, machines are becoming more independent and capable of communicating and working together on their own. Numerous studies have documented the uses of AI within process industries for predictive maintenance [30, 31], quality control [32, 33], real-time monitoring [34, 35], and energy efficiency [36, 37]. The integration of AI in the advanced exergy analysis for different operations have also been documented. O"Ozkaraca et al [38]. conducted a study in which conventional exergy analysis, advanced exergy analysis, and artificial bee colony (ABC) methods were employed to investigate the thermodynamic operation of binary geothermal power plant. The study's findings reveal that the total exergy efficiencies for these three approaches are 39.1% for conventional exergy analysis, 43.1% for advanced exergy analysis, and 42.8% for artificial bee colony method. FA Boyaghchi et al [39]. utilized advanced exergy analysis and optimization techniques for the parametric analysis of a real Combined Cycle Power Plant (CCPP) with duct burners (DB). In this work, the sensitivity of both CO<sub>2</sub> emission and total avoidable exergy destruction were evaluated concerning variations in compressor pressure ratio, DB fuel mass flow rate, and turbine inlet temperature. Furthermore, the researchers employed NSGA-II for the optimization of CCPP. The optimal values for the CO<sub>2</sub>

emissions and total avoidable exergy destruction rate exhibited improvement of 8.3%, and 10.6% respectively, compared to the source case. L Liu et al [40]. Conducted a study on a wind-solar-hydrogen multi-energy supply (WSH-MES) system. The research utilized a multi-objective optimization methodology to determine the optimal equilibrium between energy, exergy, advanced exergy, and economic factors. In another work, M Khan et al [41]. created straight run (SR), ANN models, GA to explore the effects of simulated variations in operational parameters and crude constituents on exergy efficiency.

# Chapter 3

## Process Description and Methodology

### 3.1 Process description

Figure 2 illustrates a schematic overview of the atmospheric distillation segment within the plant, comprising three primary groups, the heat exchanger network, the furnace, and the distillation column. The model was constructed using Aspen HYSYS V.11 and subsequently adjusted to align with data from the existing literature [29, 42]. The CDU is operated at 150000 barrels per day (150,000 BPD). In the production route, crude oil is flowing through the HEN before going towards the furnace. within the furnace, crude oil is subjected to heating, reaching a temperature of 371°C, which facilitates its fractionation into various products. These products include atmospheric gas oil (AGO), medium vacuum gas oil (MVGGO), heavy diesel (HDIESEL), vacuum residue (VR), and heavy vacuum gas oil (HVGGO).

The temperature differential of oil between component's inlet and temperature of the stream coming out from furnace is approximately 343 degrees, making it highly advantageous to utilize the preheat train (PHT) as an evolutionary process. By using preheat train plant energy efficiency will increase whereas the operating costs and environmental impact will be reduced. The PHT consists of twenty-five shell and tube heat exchangers, which are linked in series and parallel configurations. In PHT, the fractions derived through distillation transfer heat to oil (illustrated as the red lines in Fig. 2), which then enters furnace. As previously noted, that procedure has favourable effect on fuel utilization, leading to lower operational costs and reduced environmental effects. However, it also influences the operational expenses of products. If the heat exchanger network is not utilized, an alternative process would be necessary to lower their temperature before storing or transporting them.

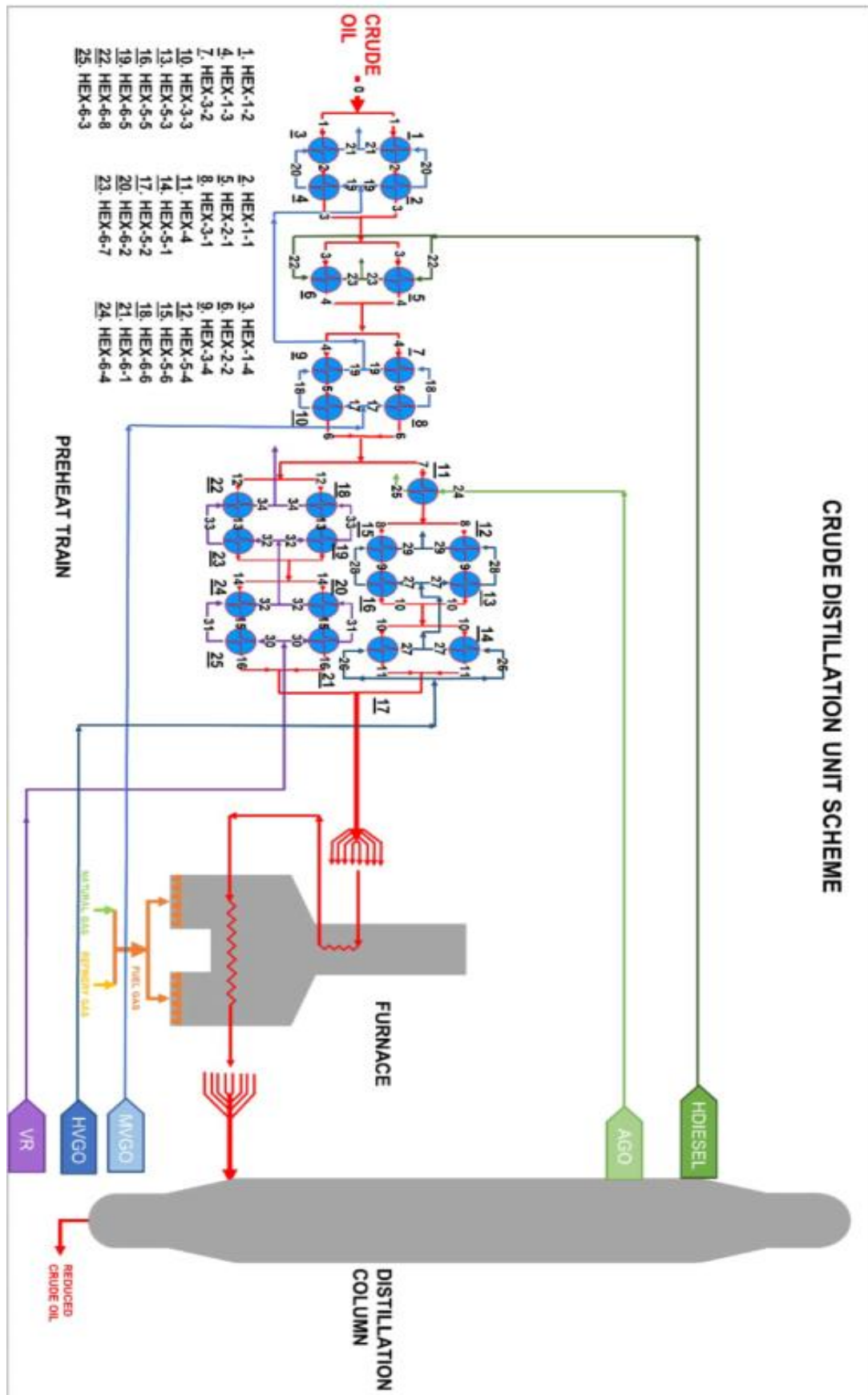


**Figure 2:** Scheme of Preheat Train of the Crude Distillation Unit [42]

### 3.2 Thermodynamic properties

The research begins with the crucial parameters, heat capacity at constant pressure ( $C_p$ ), which forms the basis for deriving the other fluid properties. Various models are available for calculating  $C_p$  as a function of temperature in the case of crude oil. However, for this study, we opted for equation 1, as proposed by Polley [43]. This choice is grounded in its superior alignment with the operational data of the specific PTH under investigation [42].

$$C_{p\text{crude oil}} = (3T + 1940)10^{-3} \quad (1)$$

The utilization of the API standard, "Technical Data Book - Petroleum Refining" [44], employed in [45], [46] facilitates the calculation of  $C_p$  for fractions obtained through distillation. Equation (2) has been adapted from the API's original formula to work within the international system's unit framework.

$$C_{p\text{fraction}} = 4.19 * 10^{-3}[A_1 + A_2(1.8T + 491.67) + A_3(1.8T + 491.67)^2] \quad (2)$$

$A_1$ ,  $A_2$ , and  $A_3$  are the characteristic constants of the fractions. They are used to classify them according to their boiling point. These constants depend upon specific gravity (SG) and Watson characterization factor ( $K_w$ ). For the calculation of these constants equations (3), (4), and (5) are employed.

$$A_1 = -1.17126 + (0.023722 + 0.024907SG)K_w + (1.14982 - 0.046535K_w)SG^{-1} \quad (3)$$

$$A_2 = (10^{-4})(1 + 0.82463K_w)(1.12172 - 0.27634SG^{-1}) \quad (4)$$

$$A_3 = (-10^{-8})(1 + 0.82463K_w)(2.9027 - 0.70958SG^{-1}) \quad (5)$$

Corresponding to thermodynamic principles, the enthalpy and entropy connected with the  $i$ -th flow in its liquid state can be calculated using the following equation:



$$h_i \approx C_p i T_i \quad (6)$$

$$s_i - s_o = \int_{T_o}^{T_i} C_p(T) \frac{dT}{T} \approx C_{p,avg} \ln \frac{T_i}{T_o} \quad (7)$$

### 3.3 Conventional exergy analysis

Exergy is a fundamental concept in thermodynamics, representing the maximum work potential that a process, substance, or system can achieve when it reaches evenness with its surroundings [47, 48]. This measure encompasses the summation of various components, including kinetic, potential, physical, and chemical exergies [25].

$$\dot{E}_K = \dot{E}_K^{PT} + \dot{E}_K^{KN} + \dot{E}_K^{PH} + \dot{E}_K^{CH} \quad (8)$$

The exergy change in HEX at any point is solely attributed to the physical alterations, with no chemical reactions taking place. Additionally, any fluctuations in potential and kinetic exergies are regarded as insignificant. The physical exergy of a particular stream is established by

$$e^{PH} = h_i - h_o - T_o(S_i - S_o) \quad (9)$$

In second-law studies, exergy is usually classified based on its role within a process. Exergy that serves as the desired output is classified as "products," and exergy that supplies the necessary inputs is denoted as "fuel" [49]. Exergy destruction represents portion of effective energy that fuel provided but was not accepted by the product. In the context of this study, the exergy contained within the crude oil is categorized as product exergy, while the exergy from the hot fluid is considered the fuel exergy.

$$\dot{E}_{DK} = \dot{E}_{F,K} - \dot{E}_{P,K} \quad (10)$$

In conventional analysis, the exergy indicators employed include exergy efficiency and exergy destruction ratio [50].

$$\varepsilon_k = \frac{\dot{E}_{P,k}}{\dot{E}_{F,k}} \quad (11)$$

$$Y_K = \frac{\dot{E}_{D,K}}{\dot{E}_{F,Total}} \quad (12)$$

### 3.4 Advanced exergy analysis

Lately, advanced exergy analysis has emerged as an innovative thermodynamic approach, greatly enhancing the abilities of exergy analysis in process evaluation. Pioneers in this field, such as Morosuk and Tsatsaronis [51, 52] have paved the way for advanced exergy analysis. Exergy analysis aids in recognizing the system elements with significant exergy destruction and the underlying activities causing it. While it's possible to enhance a component's efficiency by reducing its exergy destruction, there will always be some unavoidable exergy destruction due to technological constraints. Moreover, a portion of exergy destruction results from its accumulation in other system elements. This indicates that improving various components, not just the one with the ultimate exergy destruction, is essential. In advanced exergy analysis, exergy destruction,  $\dot{E}_{DK}$ , is separated into avoidable,  $\dot{E}_{DK}^{AV}$ , and unavoidable,  $\dot{E}_{DK}^{UN}$ , components as well as endogenous,  $\dot{E}_{DK}^{EN}$ , and exogenous,  $\dot{E}_{DK}^{EX}$ , components. This approach allows for the assessment of how component interactions and technological limitations impact a system's efficiency. A comprehensive explanation of the methodology is available in references [53-55].

#### 3.4.1 Splitting exergy destruction

Exergy destruction inside an element can be dissected into two primary components. The initial portion is related to the inner inefficiencies of the element and is termed endogenous exergy destruction. The second part arises from inefficiencies that exist in other components but have an impact on the component under examination, this is referred to as exogenous exergy destruction. In count to distinguishing between endogenous and exogenous exergy destruction, it's also feasible to categorize the overall exergy destruction into two key aspects: unavoidable exergy destruction and avoidable exergy destruction. Avoidable exergy destruction can be mitigated by enhancing component's efficiency or through the development of new

technologies. However, it's important to note that in each real element, there exist a portion of exergy destruction that cannot be realistically decreased, Figure 3. provides a graphic depiction of this exergy distribution, which aids in comprehending the extent of exergy destruction values.

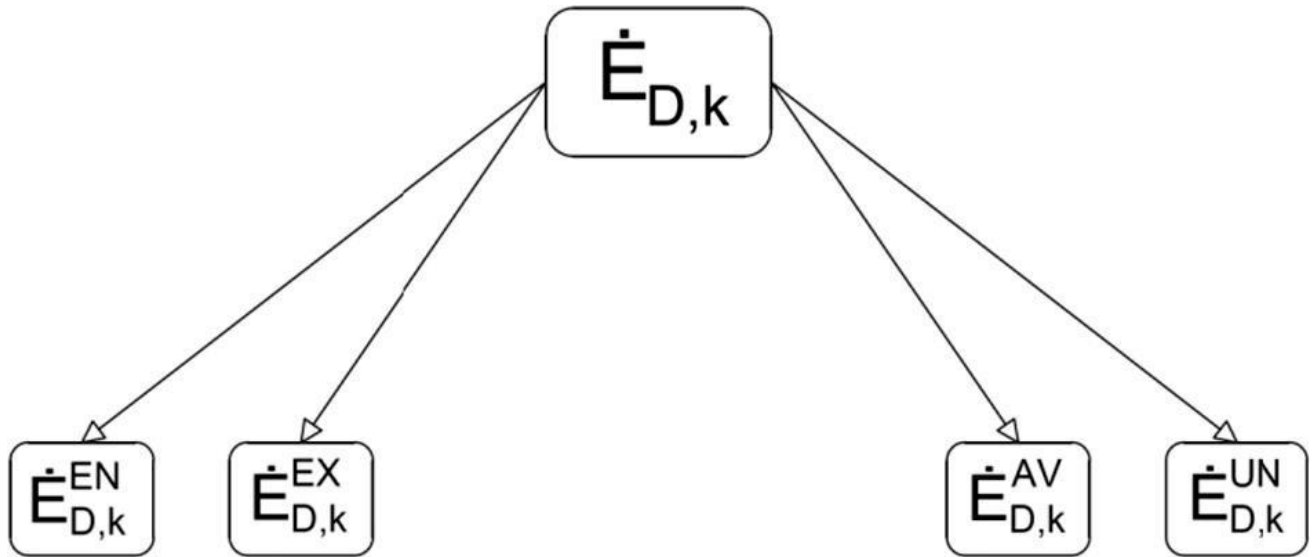


**Figure 3:** Exergy destruction splitting of a component k [56]

### 3.4.2 Avoidable and unavoidable exergy destruction

As mentioned earlier, practical and economical constraints often create difficulties that render a portion of inefficiencies unavoidable. In terms of avoidable inefficiencies, the entire exergy destruction for Kth component of a procedure is characterized as follows [57]:

$$\dot{E}_{D,K} = \dot{E}_{D,K}^{UN} + \dot{E}_{D,K}^{AV} \quad (13)$$

For the calculation of unavoidable exergy destruction ( $\dot{E}_{D,K}^{UN}$ ), the component of concern must be isolated from system, and it reasonable to assume in which it operates in accordance with most favourable circumstances, achieving its best possible performance. In this way, the quantity of specific unavoidable exergy destruction  $\left(\frac{\dot{E}_D}{\dot{E}_P}\right)_K^{UN}$  is obtained. Then obtained value is then multiplied by product of constituent, resulting in the calculation of the unavoidable exergy destruction based on actual operational circumstances [58].

$$\dot{E}_{D,K}^{UN} = \dot{E}_{P,K} \left( \frac{\dot{E}_D}{\dot{E}_P} \right)_K^{UN} \quad (14)$$

$$\dot{E}_{D,K}^{AV} = \dot{E}_{D,K} - \dot{E}_{D,K}^{UN} \quad (15)$$

Once both the avoidable and unavoidable exergy destruction have been recognised, it is more practical to utilize an amendment of exergy efficiency  $\varepsilon_k^*$ . It will give precedence to the impact of avoidable exergy destruction on the utilization of the element under observation [58].

$$\varepsilon_k^* = \frac{\dot{E}_{P,K}}{\dot{E}_{F,K} - \dot{E}_{D,K}^{UN}} \quad (16)$$

### 3.4.3 Endogenous and exogenous exergy destruction

Endogenous exergy destruction signifies exergy lost inside an element due to its own inefficiency. This is computed maintaining all other apparatuses at their best states while evaluating components in question using its real operational conditions. Exogenous exergy destruction, on other hand, is associated with inefficiencies in other equipment throughout the system. The total exergy destruction is determined in following manner [52, 59]:

$$\dot{E}_{D,K} = \dot{E}_{D,K}^{EN} + \dot{E}_{D,K}^{EX} \quad (17)$$

The central focus of advanced exergy analysis pertains to endogenous irreversibility. Two primary techniques are applied to compute endogenous irreversibility of apparatus: thermodynamics and engineering methods. The engineering technique is employed to determine the endogenous irreversibility in this study. The engineering or graph approach was initially established by Kelly et al. [56] who delivered a comprehensive explanation of the methodology and its efficiency in assessing the endogenous irreversibility of apparatus. The fundamental concept of the graph method is illustrated in Figure 4. This figure depicts alterations in the overall irreversibilities of the process equipment's in relation to the total irreversibilities of the process equipment, excluding equipment K. According to exergy balance equation, the vertical axis of graph equals total irreversibility of the procedure as below:

$$\dot{E}_{F,tot} - \dot{E}_{L,tot} - \dot{E}_{P,tot} = \dot{E}_{D,tot} \quad (18)$$

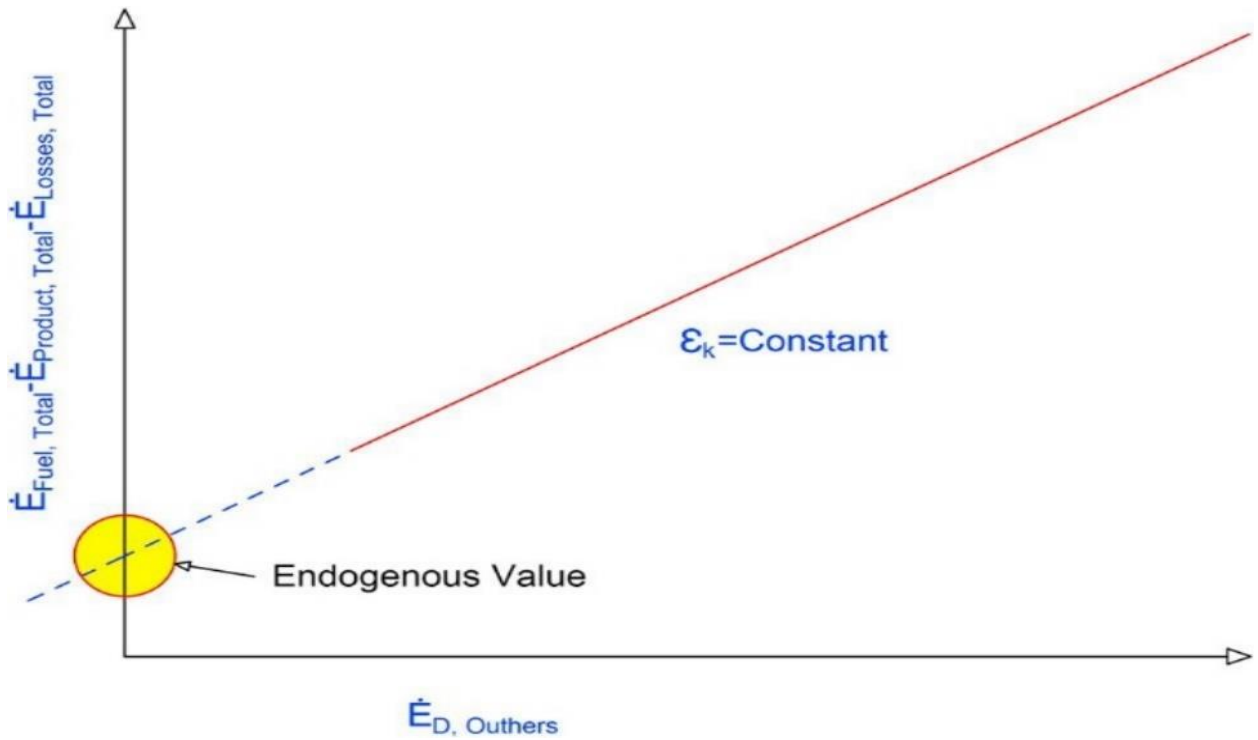


**Figure 4:** Line obtained by graphical method for endogenous exergy destruction [56]

### 3.5 Artificial neural network

Artificial neural network is a computational model compiled of multiple interconnected neurons designed to replicate human brain functionality, allowing for quantitative data interpretation through learning and training [60]. Neurons receive inputs in the form of variables and employ triggering function to compute outputs. Every input is associated with a related weight. As point out in Figure 5, neuron's output is determined through a nonlinear sequence of its inputs ( $x_1, x_2, \dots, x_n$ ) and weights ( $w_1, w_2, \dots, w_n$ ). During learning process, synaptic weights are adjusted. Learning is aimed at fine-tuning network applying a dataset in which mutually input, and output quantities are ascertainable. In the Figure 5, 'b' represents bias and 'f' denotes the activation function [61].

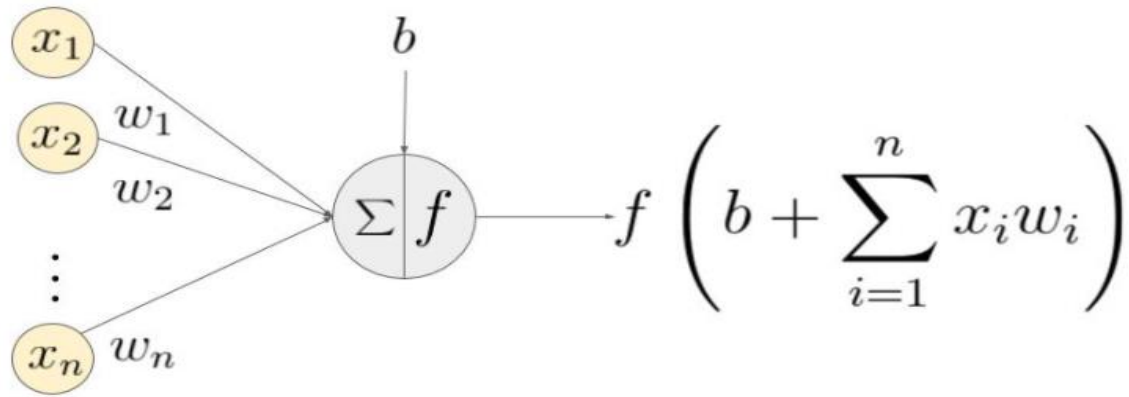


**Figure 5:** General representation of weights and biases for ANN [61]

An ANN typically contains three primary layers: input, hidden, and output. These layers contain interconnected neurons which enable the network to model complicated and nonlinear functions as illustrated in Figure 6. The input layer's role is to receive information, features, from exterior environments. Neurons within hidden layers are tasked with getting information relevant to observed process. The neurons in the output layer have the responsibility of making and revealing final outputs of network. These outputs result from the computations carried out by neurons in the previous layer [62].

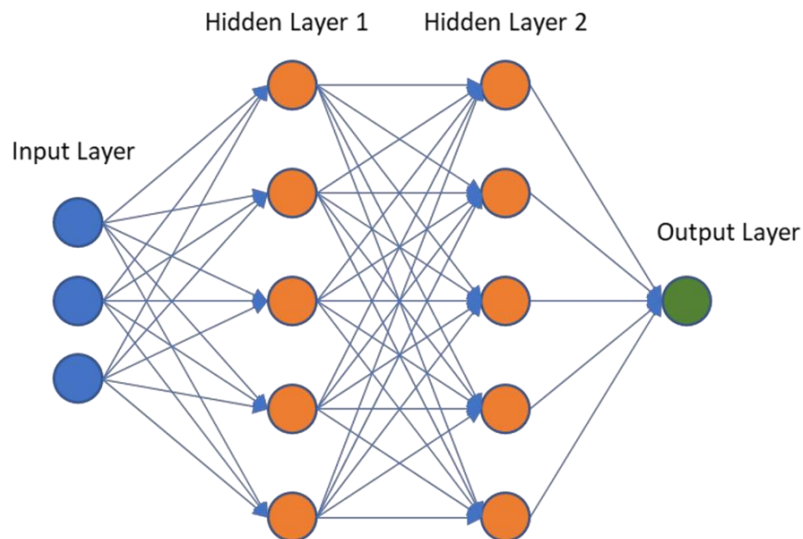


**Figure 6:** General ANN architecture [62]

### 3.5.1 The Levenberg-Marquardt method

The Levenberg-Marquardt technique is employed to resolve nonlinear programming challenges by minimizing sum of squared errors between the model function and the data points. It accomplishes this by iteratively updating a t sequence of parameters through a combination of gradient descent and the Gauss-Newton update, as indicated in equation (19).

$$[J^T W J + \lambda(J^T W J)]h_{lm} = J^T W(y - \hat{y}) \quad (19)$$

The gradient descent method minimized the sum of squared errors by adjusting the parameters in steepest descent direction. The Gauss-Newton approach, on other hand, aims to reduce the total squared errors by pretending that least squares function is close by quadratic. The value of the damping parameter ( $\lambda$ ) plays a crucial role in this process. If the dumping parameter  $\lambda$  is fixed to a modest value, the result is a Gauss-Newton update. Conversely, when  $\lambda$  is set to a large value, it leads to a gradient descent update. Initially, a large  $\lambda$  is chosen to ensure that first updates are short steps in steepest-descent path. As solution improves and the algorithm progresses,  $\lambda$  is minimized. This gradual reduction of  $\lambda$  moves the solution toward a local minimum, making the algorithm approach the Gauss-Newton method [63].

### 3.6 Genetic algorithm

Genetic algorithm is a metaheuristic method employed for solving optimization problem based on the principle of natural selection. It operated as a population-based search algorithm that incorporates the concept of survival of fittest [64]. The algorithm constantly updated population of discrete results. During each iteration, genetic algorithm creates offspring for next production. This is achieved by randomly selecting individuals from current inhabitants to work as parents, and their offspring are determined through assessment of their fitness using a fitness function. The algorithm continues to run until specific objective criteria are met. If these criteria are not satisfied, the evaluation process recurs. Over time, inhabitants gradually progresses towards best result through various processes, including selection probabilities, mutation, and crossover, as illustrated in Figure 7[65].

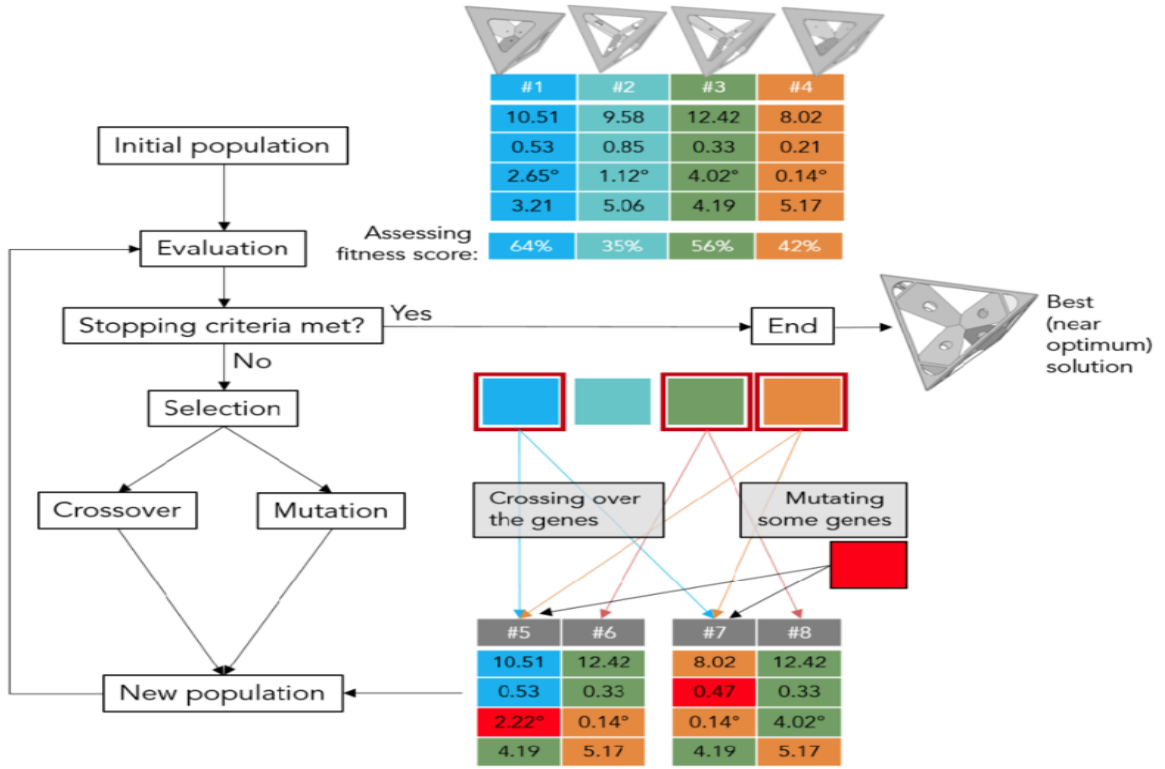


Figure 7: Schematic representation of Genetic Algorithm [66]

### 3.6.1 Genetic operators

Each genetic operator serves a specific function, which are as follows

**Population:** An initial population group was randomly generated, and each potential solution is referred to as a chromosome, as demonstrated in Table 1.

$$P = \{p_1, p_2, \dots, p_{pop-size}\} \quad (20)$$

$$p_i = [p_{i_1} p_{i_2} \dots p_{i_j} \dots p_{i_{no-vars}}] \quad (21)$$

$$para_{min}^j \leq p_{i_j} \leq para_{max}^j \quad (22)$$

Table 1: Chromosomes representation of general GA [67]

Chromosomes 1	1101100100110110
Chromosomes 2	1101111000011110



Where  $p_{pop-size}$  represent the total size of population, and  $no\_vars$  represent the number of variables to be tuned,  $para_{min}^j$  and  $para_{max}^j$  are the minimum and maximum values parameter  $p_{ij}$ .

**Selection:** In each successive generation, a subset of the current population is chosen for breeding the next generation. This selection process is based on fitness, where individual solutions are assessed for their suitability. Commonly used selection methods are roulette wheel, rank, stochastic universal sampling, and tournament. These methods help in identify feasibility of every result and ultimately select most favourable one [67].

The roulette wheel selection method, potential strings are drawn on a wheel, and a portion of the wheel's space is assigned to string based on its fitness value. Then, the wheel is spun randomly to choose a specific solution that will participate in the formation of next creation, as illustrated in Figure 8. Rank selection is an evolution of the roulette wheel method. This approach evaluates individuals based on their ranking within the population rather than their fitness and also ensures that every individual get an equal chance of being selected for the next generation.

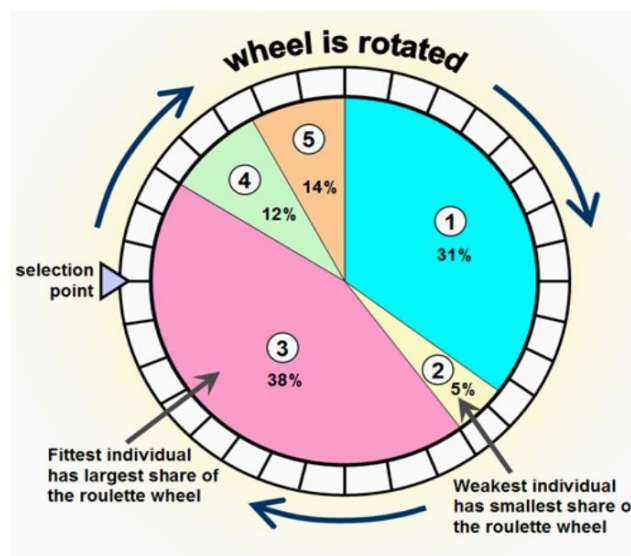


**Figure 8:** Roulette wheel selection for the population [67]

Stochastic universal sampling (SUS) is a method that select a new individual at regular spaced intervals, starting from a random point within a list of individuals from a particular generation.

This approach ensures that every individual has an equal chance of being selected. In tournament selection, individuals are selected through a stochastic roulette wheel based on their fitness values. The individual with the better fitness level is attached to pool of next creation, as depicted in Figure 9 [68].

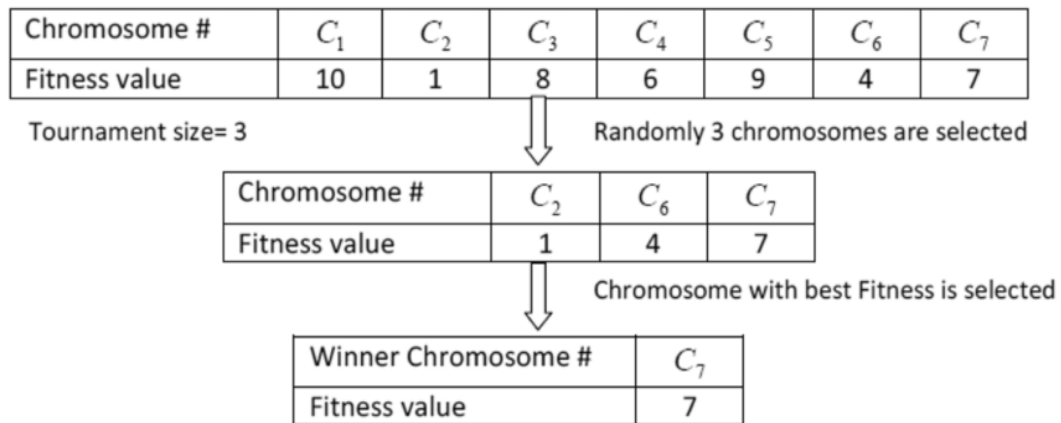


**Figure 9:** Tournament selection in GA [68]

**Crossover:** Childrens are generated by combining the genetic information of two parents from the previous generation.

In a single-point crossover, a random point is chosen, and the genetic information preceding that point is exchanged between the two parents, as depicted in Figure 10.



**Figure 10:** Single point crossover [68]

In double point crossover, two random points are chosen, and genetic information is swapped segment by segment between the parents, as demonstrated in Figure 11.



**Figure 11:** Double point crossover [68]

In the uniform crossover, each gene in parents is treated individually. Arbitrary decisions are made for each gene, determining whether it should be swapped with the corresponding gene in the other chromosomes, as illustrated in Figure 12 [69].

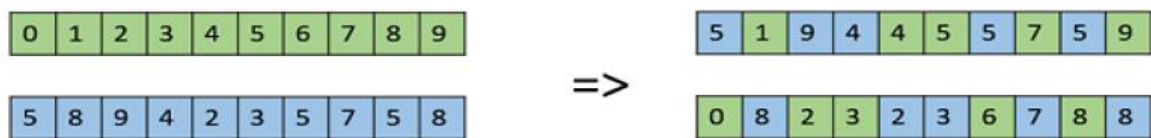


**Figure 12:** Uniform points crossover [68]

In the over scattered crossover, a random chromosome is generated, and genes are selected based on whether the chromosome is 0 from second parent or 1 from the first parent. These selected genes are then combined to form a child.

**Mutation:** Mutation is crucial for preserving genetic diversity from one population to the next. It involves making changes to the genes within chromosomes. Consequently, the characteristic of chromosomes inherited from parents may undergoes alterations. The mutation procedure will generate three additional progeny [67].

### 3.7 Particle swarm optimization

Particle swarm optimization algorithm is based on population hunt outstanding by the collective behaviour of birds in a flock. This algorithm involves a collection of individuals known as particles that relocate iteratively around a defined area. During respective phase, algorithm evaluates the objective function for each particle. The particle is then attached to the best position it has encountered so far, either within its own trajectory or the best position discovered by any member of the swarm. After some steps, the swarm may converge to a single

location or disperse across several locations. After the estimation, the algorithm computes new velocities for every particle, and the algorithm is iteratively repeated as depicted in Figure 13.

- The algorithm initiates by creating initial particles and assigning them their initial velocity.
- The best location and function value are determined by evaluating the objective function at each particle's location.
- New particle velocities are selected based on combination of the current velocity, and best location of individual particle, and the best location among neighbouring particles.
- The algorithm iteratively repeats the entire process until the specified objective criteria are satisfied.

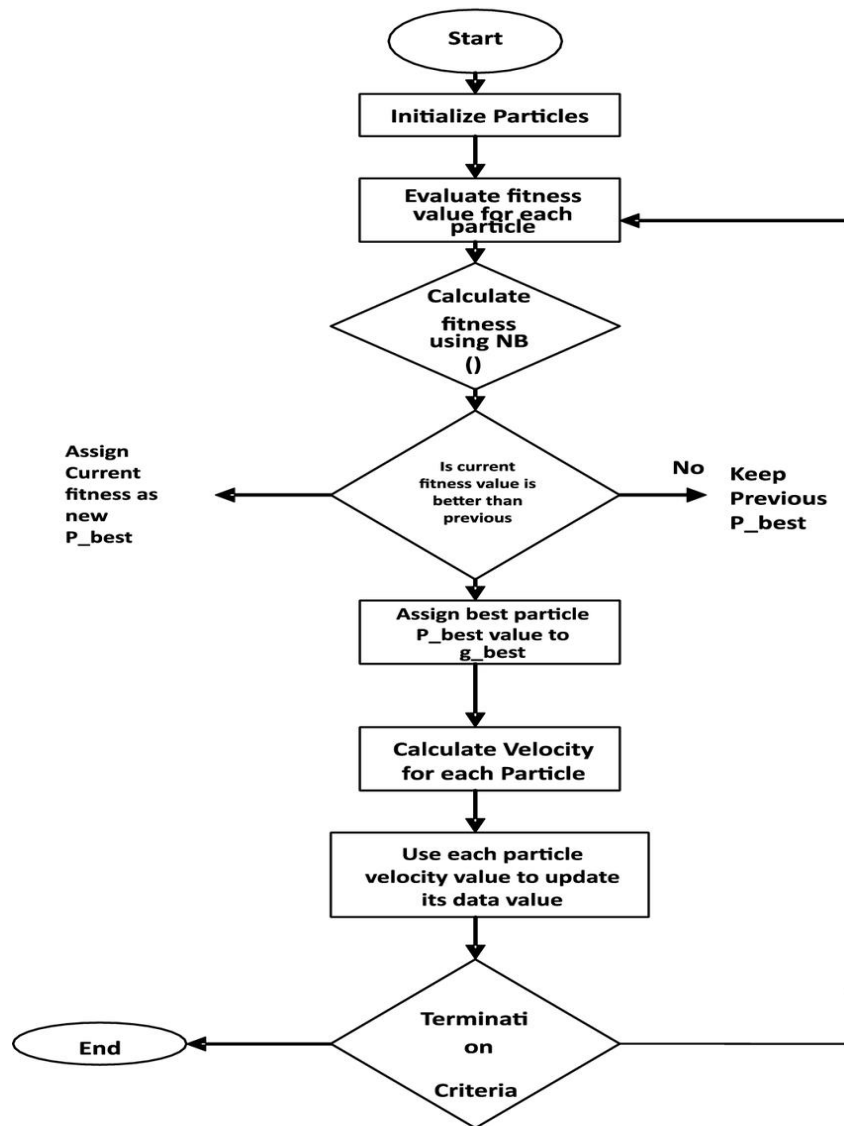


Figure 13: Workflow of particle swarm optimization

### **3.8 Surrogate model**

The surrogate model is an analytical approach used to establish static relationships between the inputs and output behaviours of complex systems, it's also referred to as a meta-model. Surrogate models are categorized into two types based on their approximation strategy: model-driven and data-driven or black box. In model-driven surrogate models, often referred to as Reduce Order Model (ROM), computational costs are reduced by utilizing lower order equations to approximate the original ones. However, this approach typically requires access to the source code of the simulator, which can be challenging when working with commercial software. Conversely, in a data-driven surrogate model, the model is generated using input data and corresponding output responses, making it a versatile approach that does not rely on access to source code.

The development of a surrogate model involves the following steps

1. The design space is systematically sampled to determine the input parameters for data sets.
2. The simulator is executed, or experiments are conducted to compute the outputs corresponding to the input parameters.
3. A surrogate model is chosen and trained using training data, which consist of input-output pairs.
4. The model's performance is assessed using test data. If the model's accuracy is found to be unsatisfactory, the entire process repeats from step 1 [70].

### **3.9 Methodology**

A succinct overview of the research approach employed in this study is presented in Figure 14. The methodology comprises five primary steps, each of which is succinctly outlined below:

#### **3.9.1 Phase-I: Steady-state conventional and advanced exergy analysis**

The following assumptions and conditions were considered for the analysis:

- All processes were evaluated in a steady state.

- Kinetic and potential exergies were considered insignificant.
- The reduction in mass flow due to material accumulation on the exchanger walls was considered negligible.
- Dead state conditions were assumed to have a temperature of 25 °C and a pressure of 101.325 kPa.
- For the unavoidable conditions, design energy efficiency was obtained from the datasheet.
- Energy Efficiencies for the theoretical condition were calculated by increasing the values from the unavoidable condition by 20%, higher increments resulted in an excessive rise in the furnace inlet temperature.

**Table 2:** Real, Unavoidable and Theoretical condition for each Heat Exchanger

<b>HEX</b>	<b>Real <math>\eta(\%)</math></b>	<b>Unavoidable <math>\eta(\%)</math></b>	<b>Theoretical <math>\eta(\%)</math></b>
1-1/3	40.47	56.48	67.78
1-2/4	53.47	60.72	72.87
2-1/2	39.64	59.62	71.54
3-1/3	37.36	57.96	69.55
3-2/4	32.28	54.55	65.46
4	19.17	26.97	32.36
5-1/2	43.07	75.57	90.68
5-3/5	29.23	35.03	42.03
5-4/6	43.99	64.53	77.44
6-1/3	40.59	48.85	58.62
6-2/4	34.76	51.57	61.88
6-5/7	40.42	51.76	62.11
6-6/8	38.30	49.00	58.80

The physical exergy of the steam streams was determined using the property data from Aspen Hysys V.11. Subsequently, with the values of physical exergy, the exergy destruction for every heat exchanger and for the overall network was determined using equation (10). Additionally, the exergy efficiency and exergy destruction ratio for each heat exchanger and the overall network were computed using equations (11) and (12). Furthermore, the exergy destruction was further categorized into avoidable, unavoidable, endogenous, and exogenous exergy destruction components. The endogenous exergy destruction was calculated using an engineering method with theoretical conditions, while for the calculation of exogenous exergy

destruction equation (17) was employed. To calculate the avoidable and unavoidable exergy destruction, equations (14) and (15) were applied with unavoidable conditions.

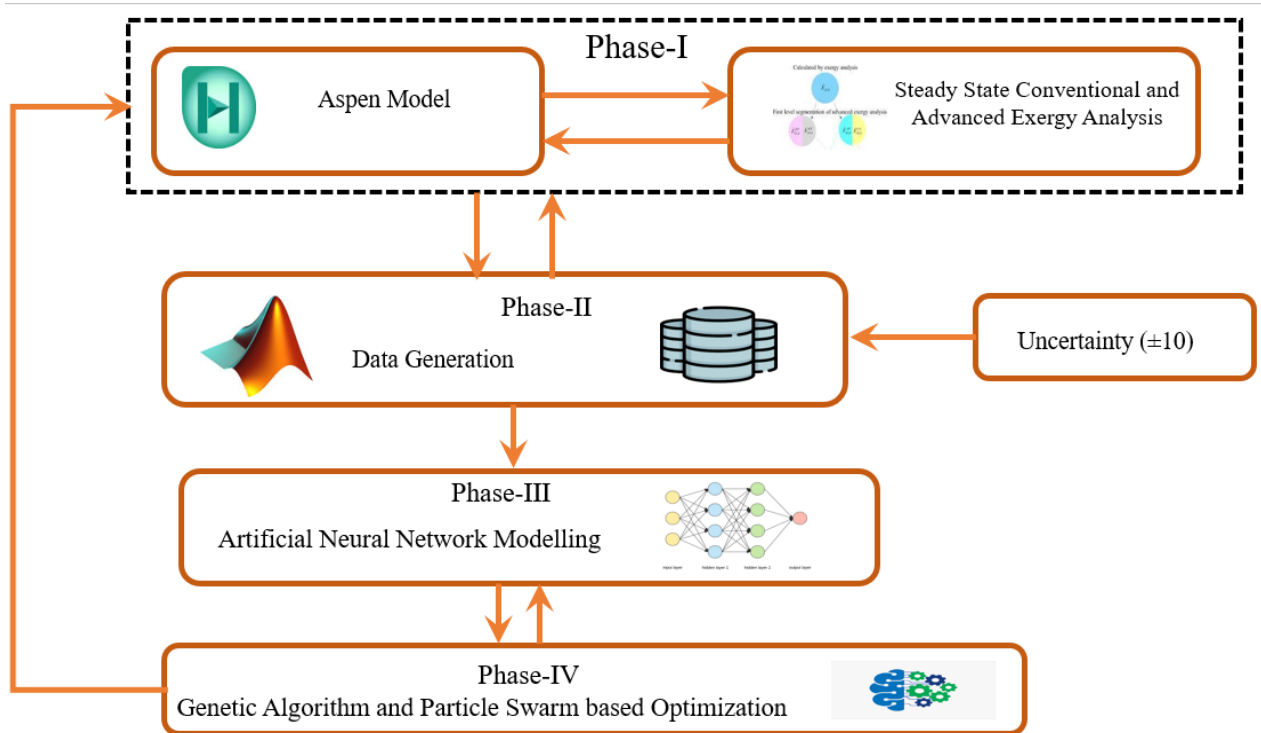


**Figure 14:** Methodology in this research

### 3.9.2 Phase-II: Data generation

A framework was created between MATLAB and Aspen HYSYS utilizing the COM actxserver to produce data samples. A dataset of 600 samples was created by transitioning the operational model to a dynamic mode and introducing  $\pm 10\%$  variability in operational parameters, including temperature, and mass flow rate. Subsequently, the overall exergy destruction and exergy efficiency, along with unavoidable and avoidable exergy destruction, and modified exergy efficiency were computed for each data sample.

**Table 3:** Some Data Samples after uncertainty

Process Conditions		Data Sample 1	Data Sample 2	Data Sample 3	Data Sample 4	Data Sample 5	Data Sample 6
Temperature °C	Crude Inlet Temp	28	29.762	30.560	29.000	29.091	30.068
	HDiesel Inlet Temp	293.55	271.650	311.17	307.82	319.98	296.47
	MVGO Inlet Temp	242.05	248.457	238.26	249.57	239.08	259.140
	AGO Inlet Temp	329.55	314.950	348.80	343.13	347.05	319.72
	HVGO Inlet Temp	332.05	362.433	342.39	317.23	311.25	325.52
	VR Inlet Temp	332.85	310.057	356.09	306.03	329.22	315.53
Mass Flow rate (Kg/hr)	Crude Inlet Flowrate	396072	428216	394913	416488	381583	402385
	HDiesel Inlet Flowrate	127116	137625	118011	124376	115280	118089
	MVGO Inlet Flowrate	252108	231815	273070	235528	246136	258262
	AGO Inlet Flowrate	118692	119804	129599	107578	125699	119006
	HVGO Inlet Flowrate	173592	189732	157472	157835	173236	158870
	VR Inlet Flowrate	122328	133841	132945	130241	125907	113112

### 3.9.3 Phase-III: ANN modelling

An ANN model was built and validated in MATLAB 2023a. The modelling process involves three key steps: model selection, training, and validation.

**Model selection:** A feed-forward neural network was chosen for modelling, employing the Levenberg-Marquardt backpropagation (trainlm) training algorithm. The dataset was partitioned in such a way that 70% of the samples were allocated for training, while the remaining 30% were evenly distributed between model validation and testing.

**Training and validation:** Model was validated by utilizing the root-mean-squared error (RMSE) and relation coefficient (R).



RMSE and R were computed based on equations (23) and (24) respectively.

$$RMSE = \sqrt{\frac{1}{n} \sum_i^n (Y_i^{exp} - Y_i)^2} \quad (23)$$

$$R = 1 - \frac{\sum_{i=0}^n (Y_i^{exp} - Y_i)}{\sum_i^n (Y_i^{exp} - Y_{avg}^{exp})} \quad (24)$$

where n is the total number of samples,  $Y_i^{exp}$  represents the actual value of the output, and the predicted value is represented by  $Y_i$ .

#### 3.9.4 Phase-IV: Optimization

The ANN model served as a surrogate in a GA and PSO framework for optimization under uncertainty, with the objective function being exergy efficiency. Both GA and PSO were employed to identify the optimal parameter that maximize exergy efficiency. The GA algorithm steps are as follows,

1. The algorithm commences by creating a set of random populations, each indicates an individual solution.
2. Fitness evaluations are conducted for each individual within the population using a surrogate model and rank them according to their respective fitness values.
3. Based on these fitness value, parents are selected for the purpose of generating offspring through the application of a crossover operator.
4. Mutation operators are employed to both enhance solution quality and maintain genetic diversity in the succeeding generation.
5. The algorithm proceeds until the criteria defined by the objective function are met. Otherwise, steps 2-4 are repeated until an optimal solution is attained.

The PSO algorithm steps are as follows,

1. The algorithm begins by generating initial particles and assigning them initial velocity.
2. A surrogate model is employed to assess the particle's position.
3. If the current position is superior to the previous one, the new personal best is updated.

4. The updated personal best is then assign as the global best.
5. The algorithm selects new particle velocities based on current velocity and best positions of individual and neighboring particles.
6. Steps 2 to 5 are iteratively repeated until the stopping criterion is met.

The efficiency of the proposed optimization was verified by running the Aspen HYSYS model with the optimized results and computing the absolute error.

# Chapter 4

## Results and Discussion

Segments 4.1 and 4.2 cover the steady-state conventional and advanced exergy assessment of preheat train in crude oil distillation column unit. Section 4.3 focuses on data-based modelling and while section 4.4 delves into the optimization using GA and PSO algorithms. Table 4 provides the operational parameters and thermodynamic characteristics of every heat exchanger stream.

**Table 4:** Characteristics for each state within the preheat train

State	Substance	T(C)	$m \frac{kg}{s}$	$e \frac{kJ}{kg}$	$\dot{E}$ (kW)
1	Crude	28	110.02	0.823	45.28
2	Crude	82	110.02	11.45	630.3
3	Crude	110.3	110.02	24.26	1334.92
4	Crude	140.4	110.02	42.94	2362.55
5	Crude	154.3	110.02	53.27	2930.506
6	Crude	174.3	110.02	71.36	3925.93
7	Crude	174.29	55.01	71.367	3925.933
8	Crude	186.5	55.01	91.76	2524
9	Crude	210.7	55.01	132.99	3658
10	Crude	226.2	55.01	160.92	4426.29
11	Crude	254.5	55.01	209.592	5764.84
12	Crude	174.29	55.01	71.36	1962.96
13	Crude	176.5	55.01	80.568	2216.034
14	Crude	183.699	55.01	96.568	2656.116
15	Crude	193.8	55.01	116.05	3191.96
16	Crude	218.4	55.01	155.77	4284.48
17	MVGO	242.05	35.015	185.73	6503.498
18	MVGO	208.37	35.015	149.475	5233.86
19	MVGO	185.549	35.015	127.27	4456.46
20	MVGO	166.114	35.015	90.775	3178.518
21	MVGO	126.183	35.015	35.53	1244.164
22	HDiesel	293.55	17.65	218.54	3858.42
23	HDiesel	217.72	17.65	117.48	2074.2
24	AGO	329.55	32.97	276.51	9116.648
25	AGO	298.67	32.97	226.99	7483.93
26	HVGO	332.05	24.1	327.117	7886.79
27	HVGO	305.68	24.1	255.54	6161.2
28	HVGO	284.42	24.1	213.552	5148.75
29	HVGO	247.319	24.1	154.384	3722.2
30	VR	332.85	16.99	280.49	4765.54
31	VR	274.63	16.99	189.99	3228.078

32	VR	242.68	16.99	146.81	2494.32
33	VR	215.616	16.99	114.039	1937.52
34	VR	199.628	16.99	96.39	1637.67

#### 4.1 Steady-state exergy analysis

The preheat train incurs an exergy destruction of 5403.16 kW, resulting in an exergy efficiency of 66.16%. Notably, seven heat exchangers exhibit significantly higher exergy destruction rates compared to the others. These include HEX-1-1/3 (two in parallel), HEX-1-2/4 (two in parallel), HEX-2-1/2 (two in parallel), and HEX-4. These heat exchangers are situated between the states of the crude line 1-3, 3-4, and 7-8, as depicted in Figure 2. Detailed exergy destruction rates and traditional exergy statistics for all heat exchangers can be found in Table 5. Figure 15 provides a breakdown of the exergy destruction contributions from each heat exchanger. Notably, HEX 1-2/4 and HEX-2-1/2 exhibit the greatest percentages of exergy destruction. In contrast, HX-6-6/8 and 6-5/7 contribute less than the average exergy destruction. Consequently, when ranking enhancement activities, targeting the latter four exchangers individually may not result in significant network performance enhancements. However, focusing on HEX-1-2/4 and HEX-2-1/2 could lead to more substantial improvements in the system.

**Table 5:** Exergy Destruction, Exergy Efficiency, and Exergy Destruction Ratio

HEX	$\dot{E}_D(\text{kW})$	$\epsilon_k(\%)$	$Y_K(\%)$
1-1/3	573.32	55.13	3.59
1-2/4	1349.33	30.243	8.45
2-1/2	756.559	57.59	4.73
3-1/3	274.204	78.402	1.717
3-2/4	209.435	73.059	1.311
4	510.6	68.72	3.19
5-1/2	387.038	77.57	2.423
5-3/5	243.715	75.917	1.526
5-4/6	292.54	79.49	1.832
6-1/3	444.956	71.059	2.786
6-2/4	197.89	73.029	1.239
6-5/7	116.739	79.033	0.731
6-6/8	46.787	84.3966	0.293

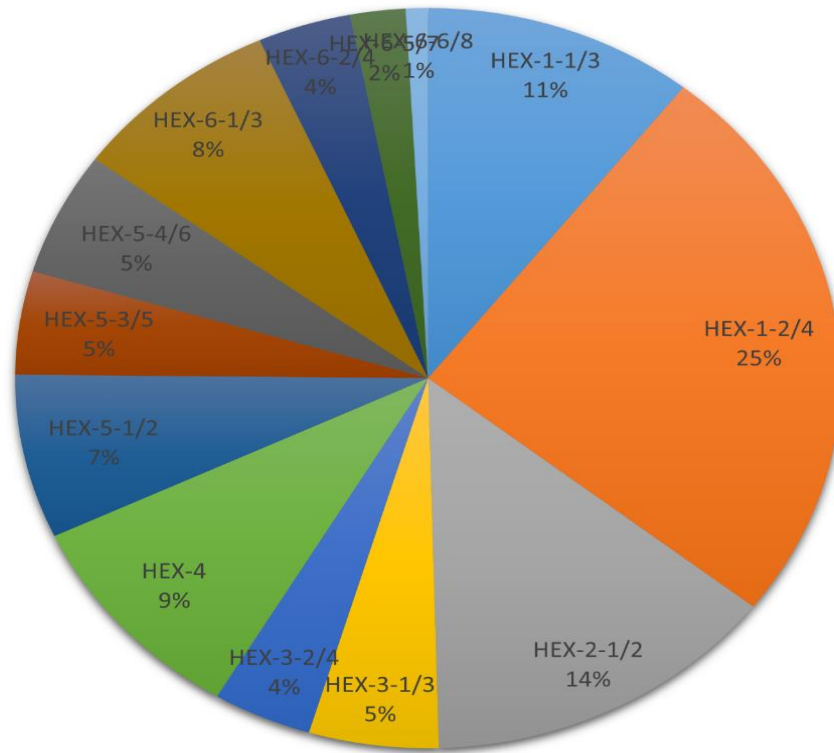


**Figure 15:** Exergy Destruction Percentage

## 4.2 Steady-state advanced exergy analysis

The assessment of avoidable and unavoidable exergy destruction revealed that only 33% of the exergy destruction is potentially recoverable. This destruction is primarily attributed to fouling inside the heat exchangers. To identify key heat exchangers, a criterion is applied, considering avoidable exergy destruction as both a selection criterion and a limit on the number of selected exchangers, which is set at 20% of the total. Exchangers whose irreversibilities affect the key heat exchangers are not classified as crucial, instead, they are recognized as contributors to the inefficiency of the key heat exchanger under examination. HEX-1-2/4 and HEX-2-1/2 stand out as the primary contributors to avoidable exergy destruction (as indicated in Figure 17), making them the key exchangers where improving operating conditions can lead to a reduction of 841.67 kW. This reduction is substantial when evaluated to the total avoidable exergy destruction across the entire network, which amounts to 1759.807 kW. Consequently, these four exchangers are designated as the key heat exchangers in the process.

**Table 6: Avoidable and Unavoidable Exergy Destruction**

HEX	$\left(\frac{\dot{E}_D}{\dot{E}_P}\right)^{UN}$	$\dot{E}_{P,K}$ (KW)	$\dot{E}_{D,K}$ (KW)	$\dot{E}_{D,K}^{UN}$ (KW)	$\dot{E}_{D,K}^{AV}$ (KW)
1-1/3	0.619	704.622	573.32	436.381	136.94
1-2/4	1.32	585.022	1349.332	772.308	577.024
2-1/2	0.478	1027.628	756.559	491.9093	264.65
3-1/3	0.2059	995.427	274.204	205.0478	69.156
3-2/4	0.1377	567.968	209.435	78.265	131.1707
4	0.35387	1122.079	510.634	397.079	113.554
5-1/2	0.1685	1338.547	387.038	225.55	161.487
5-3/5	0.2469	768.288	243.715	189.729	53.985
5-4/6	0.1396	1134.001	292.543	158.337	134.205
6-1/3	0.327	1092.514	444.956	358.119	86.837
6-2/4	0.2648	535.853	197.896	141.9087	55.987
6-5/7	0.2204	440.0598	116.739	97.015	19.724
6-6/8	0.169	253.067	46.787	42.983	3.804

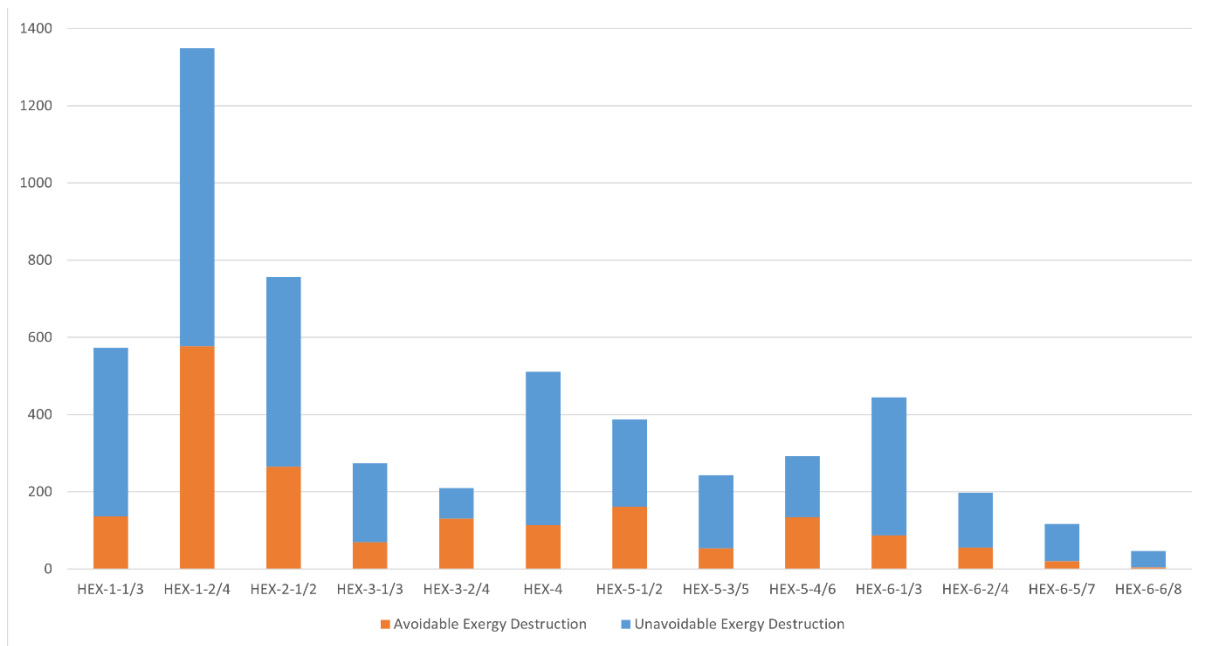


**Figure 16: Avoidable and Unavoidable Exergy Destruction**

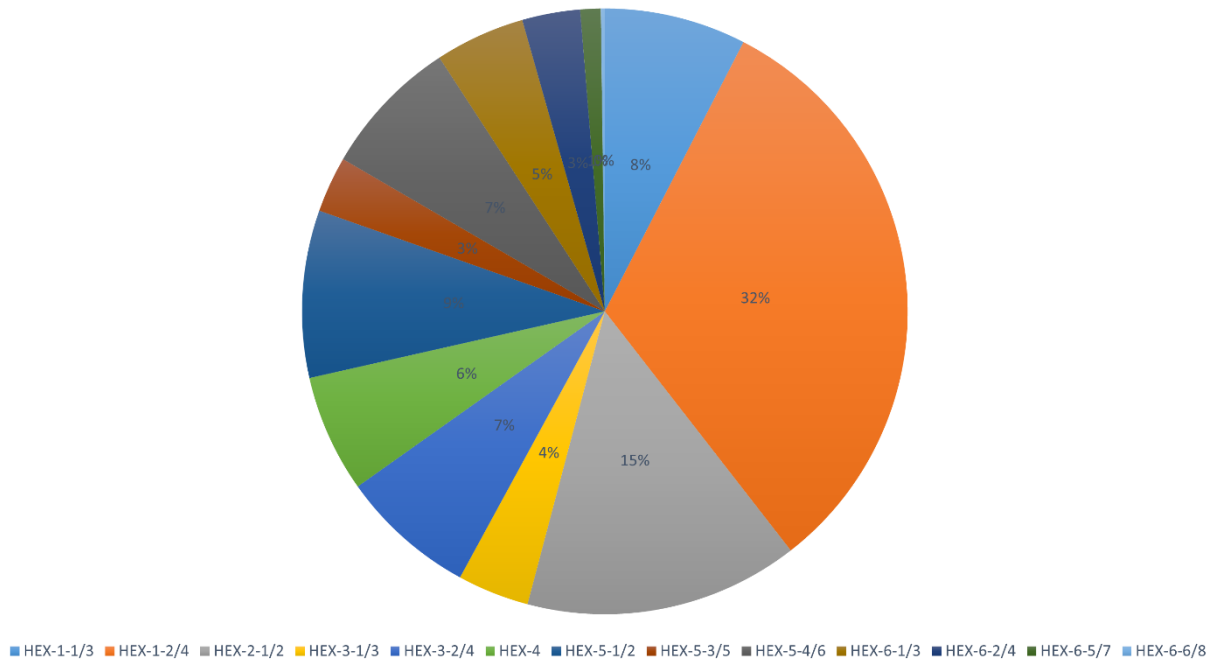


**Figure 17:** Avoidable Exergy Destruction of Heat Exchangers

Evaluating both the avoidable and unavoidable exergy destruction offers valuable insights into the heat exchangers most susceptible to fouling. As depicted in figure 16, the larger the gap between unavoidable exergy destruction and avoidable exergy destruction, the more significant the fouling impact on the heat exchangers. To assess the influence of unavoidable exergy destruction on exchanger efficiency, a comparison is made between  $\varepsilon_k$  and  $\varepsilon_k^*$ , as shown in Figure 18.

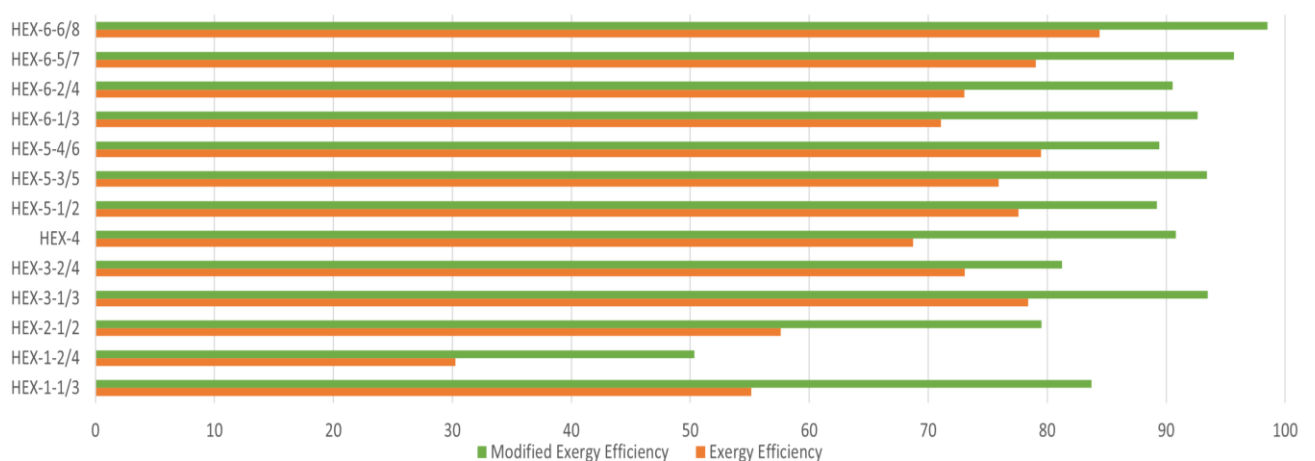


**Figure 18:** Effect of Avoidable Exergy Destruction on Exergy Efficiency

Exogenous exergy destruction with negative values as depicted in Figure 19, suggest that operating the k-component at its theoretical conditions significantly enhanced its performance. HEX-2-1/2 and HEX-4 exhibit positive exogenous exergy destruction, with worth of 210.63 kW and 123.25 kW, respectively.

**Table 7:** Endogenous and Exogenous Exergy Destruction

HEX	$\dot{E}_D$ (kW)	$\dot{E}_{D,K}^{EN}$ (kW)	$\dot{E}_{D,K}^{EX}$ (kW)
1-1/3	573.32	1394.3	-820.97
1-2/4	1349.33	2374.2	-1024.86
2-1/2	756.559	545.92	210.6397
3-1/3	274.204	1036.8	-762.595
3-2/4	209.435	608.3	-398.864
4	510.6	387.38	123.254
5-1/2	387.038	887.18	-500.14
5-3/5	243.715	952.93	-709.214
5-4/6	292.54	372.32	-79.776
6-1/3	444.956	1264.1	-819.143
6-2/4	197.89	481.67	-283.773
6-5/7	116.739	236.29	-119.55
6-6/8	46.787	109.43	-62.642

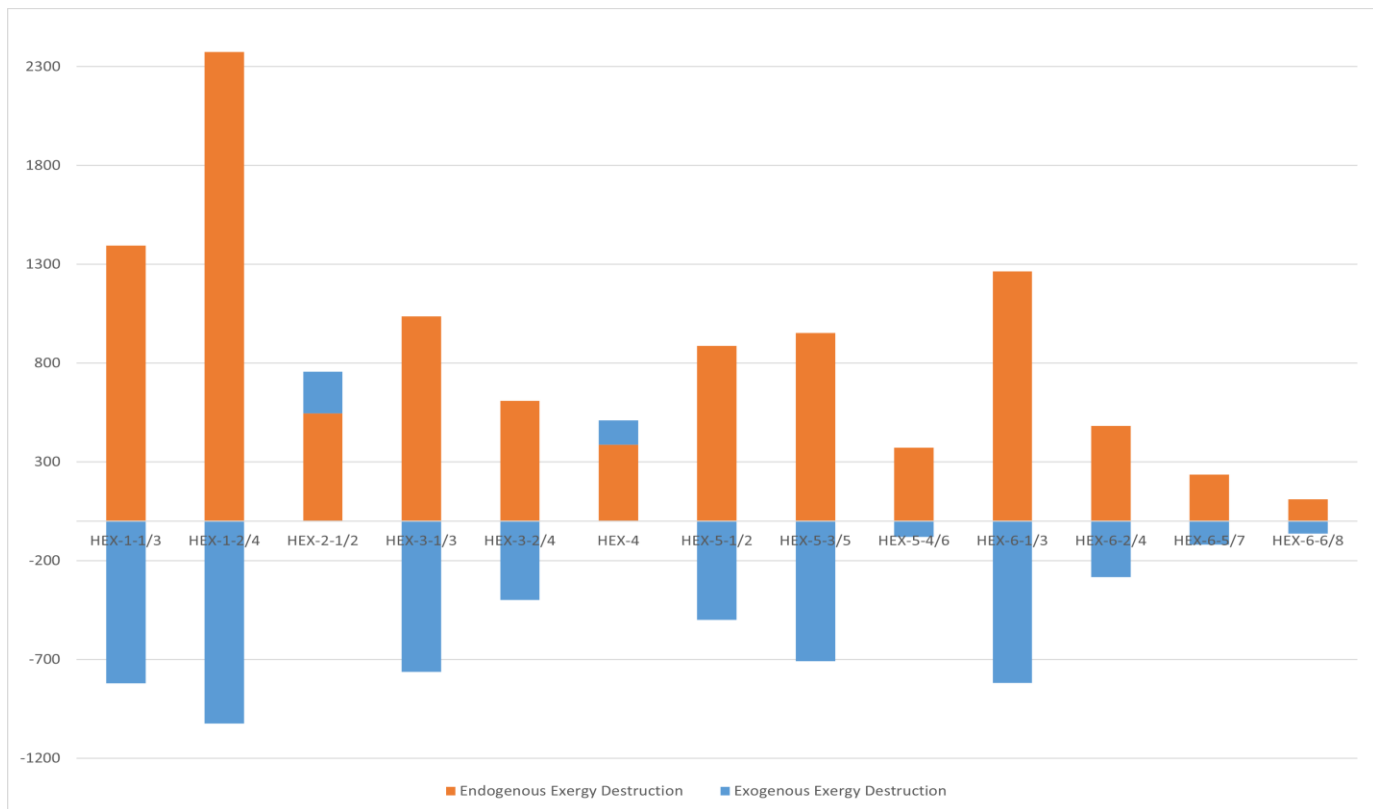


**Figure 19:** Endogenous and Exogenous Exergy Destruction



### **4.3 Data based modelling**

The steady-state traditional and advanced exergy analysis was implemented in the previous section. However, in this section, uncertainty was introduced in process parameters, and various data samples were generated. For data samples, input was uncertainty in process parameters and outputs were exergy destruction, exergy efficiency, avoidable exergy destruction, unavoidable exergy destruction, and modified exergy efficiency. Subsequently, five ANN models were constructed using the generated data samples. Each of these ANN models predicts a specific output variable while employing the same set of input parameters.

#### **4.3.1 ANNs development**

There were five ANN models were built in MATLAB 2023a. For uncertainty, variations of +10% and -10% were introduced into 12 uncertain inlet flow rates and temperatures of the inlet streams of HEN. In total, 600 data samples were generated, with 336 utilized for model training, 72 for validation, and 72 for model testing. The ANN models were trained using the Levenberg-Marquardt backpropagation (trainlm) training algorithm, and the behaviour of the networks was regulated using the Tansig activation function. To evaluate their generalization, an additional set of 120 test samples was reserved, unbeknownst to the models.

#### **4.3.2 Exergy efficiency**

This ANN model predicts the overall exergy efficiency of HEN. The ANN model demonstrated an R value of 0.99635 during training phase and an R of 0.992 during the testing phase, as depicted in the figure below.

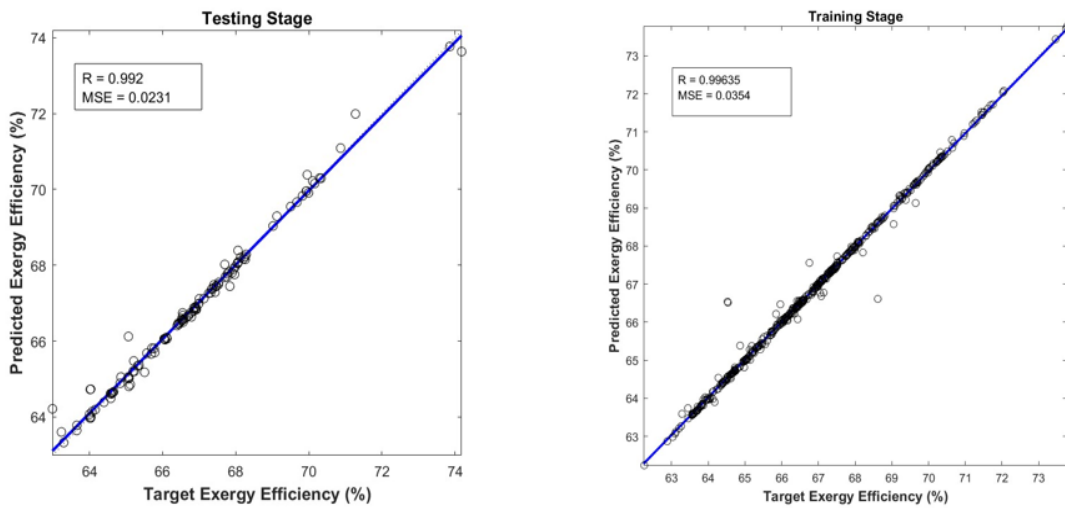


**Figure 20:** Predicted vs actual exergy efficiency of Heat Exchanger Network

### 4.3.3 Exergy destruction

This ANN model predicts the overall exergy destruction of HEN. The ANN demonstrated an R value of 0.99561 during the training phase and an R value of 0.99266 during the testing phase, as depicted in the figure below.

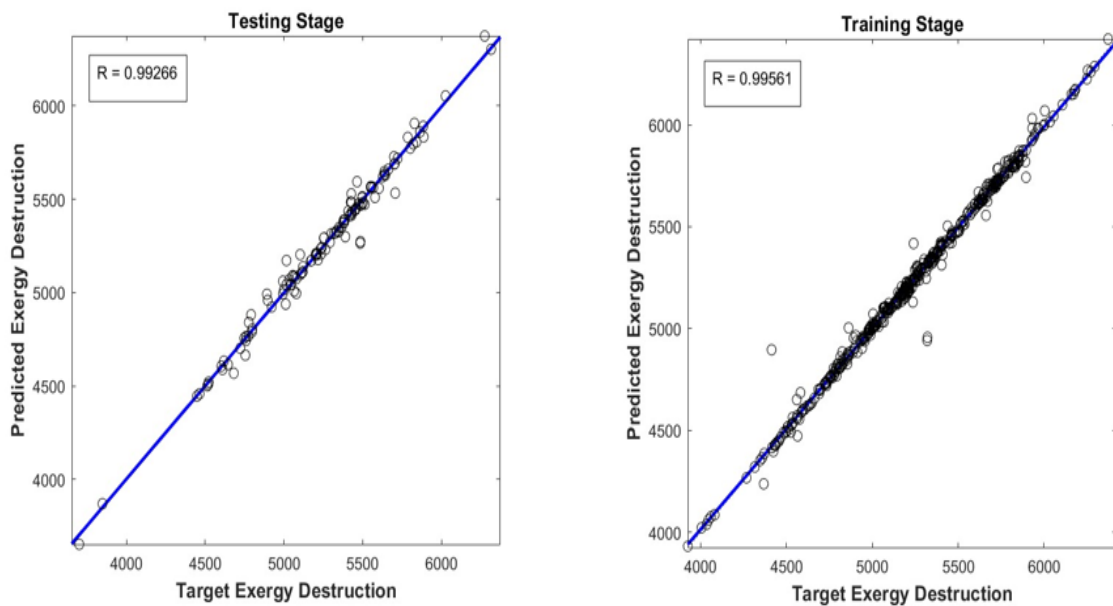


**Figure 21:** Predicted vs actual exergy destruction of heat exchanger network

#### 4.3.4 Avoidable exergy destruction

This ANN model predicts the avoidable exergy destruction of HEN. The ANN model demonstrated an R value of 0.9964 during the training phase and an R value of 0.9829 during the testing phase as depicted in the figure below.

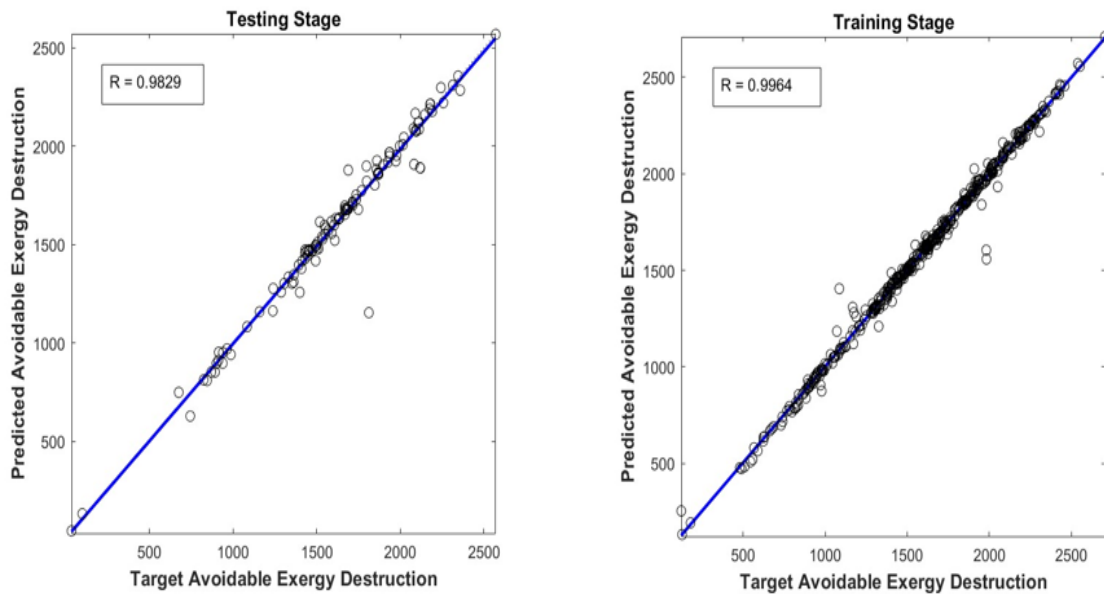


**Figure 22:** Predicted vs actual avoidable exergy destruction of heat exchanger network

#### 4.3.5 Unavoidable exergy destruction

This ANN model predicts the unavoidable exergy destruction of HEN. The ANN model demonstrated an R value of 0.99989 during the training phase and an R value of 0.99243 during the testing phase, as depicted in the figure below.

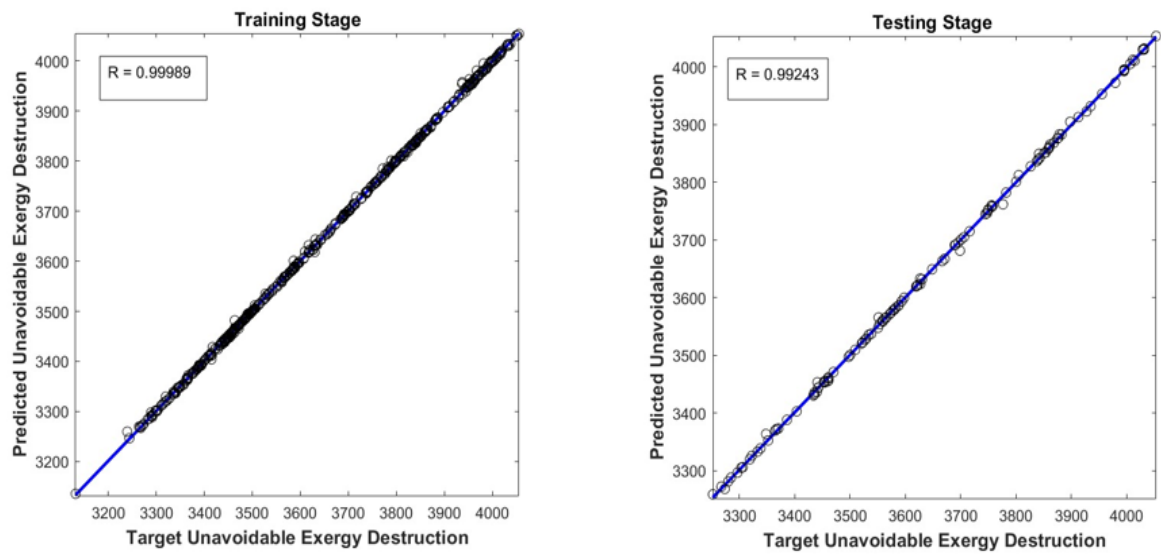


**Figure 23:** Predicted vs actual unavoidable exergy destruction of heat exchanger network

#### 4.3.6 Modified exergy efficiency

This ANN model predicts the modified exergy destruction of HEN. The ANN model demonstrated an R value of 0.99651 during the training phase and an R value of 0.99135 during the testing phase as depicted in the figure below.

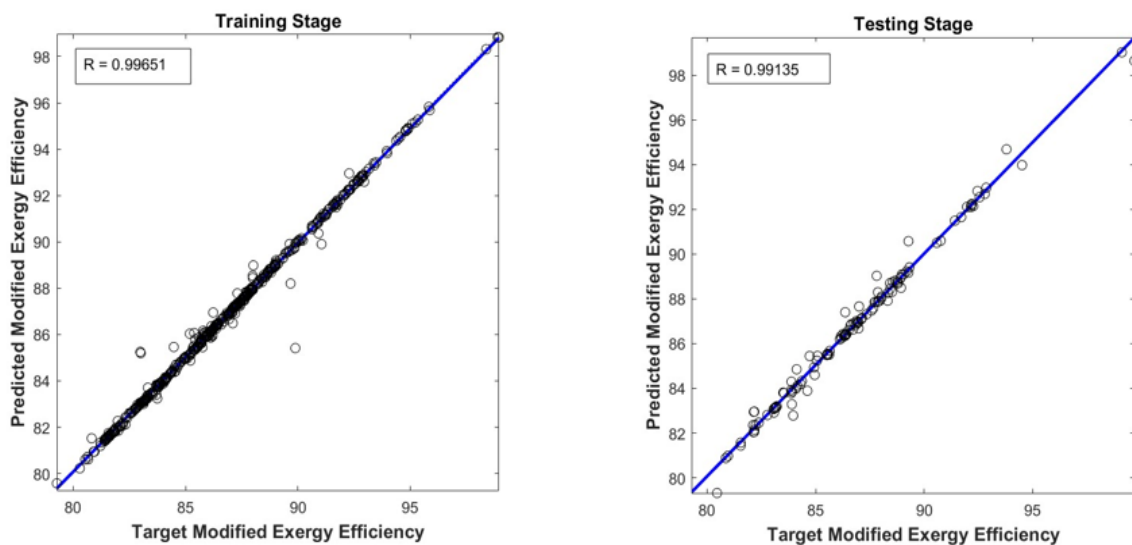


**Figure 24:** Predicted vs actual modified exergy efficiency of heat exchanger network

## 4.4 Optimization

Both the PSO and GA employ an ANN trained model as a substitute to optimize the exergy efficiency when faced with uncertain process conditions. Table 8 and Table 9 provide the parameters employed by GA and PSO for optimizing the process exergy efficiency.

**Table 8:** Genetic algorithm parameters used to optimize the exergy efficiency

<b>GA Parameters</b>	<b>Heat Exchanger Network</b>
Initial Population	100
Crossover	Over Scatter
Crossover Probability	0.8
Elite Member	15
Mutation	Adapt Feasible
Selection	Tournament

**Table 9:** PSO parameters used to optimize the exergy efficiency

<b>PSO Parameters</b>	<b>Heat Exchanger Network</b>
Swarm Size	200
Min Neighbours Fraction	0.25
Self-Adjustment Weight	1.49
Social Adjustment Weight	1.49
Initial Swarm Span	2000

### 4.4.1 Optimization of exergy efficiency of heat exchanger network:

Table 10 provide a comparison of the process's exergy efficiency across three different frameworks: standalone (SA), PSO and GA constructed frameworks. The unoptimized default Aspen's model under uncertain conditions is referred to as SA model. In all test data samples, both the PSO and GA based frameworks demonstrated superior performance compared to the SA model in spans of exergy efficiency. For instance, in data sample 1, the SA model reveals an exergy efficiency of 67.76%, whereas the PSO and GA optimization improved it to 73.77% and 73.71%, respectively. Similarly, in data sample 2, the SA model achieved an exergy efficiency of 66.10%, but both the PSO and GA optimize it to 71.75% and 71.87%, respectively.

**Table 10:** Comparison of SA, GA, and PSO exergy efficiency of heat exchanger network

SR No.	SA exergy efficiency (%)	GA optimize exergy efficiency (%)	PSO optimize exergy efficiency (%)
Data Sample 1	67.76	73.77	73.71
Data Sample 2	66.10	71.75	71.87
Data Sample 3	63.65	68.98	73.12
Data Sample 4	64.06	68.55	70.19
Data Sample 5	64.66	69.92	69.14
Data Sample 6	64.39	69.45	68.67
Data Sample 7	66.75	73.00	72.30
Data Sample 8	65.11	70.18	69.93
Data Sample 9	65.56	72.29	69.54
Data Sample 10	64.64	70.69	70.81

The framework's performance was rigorously assessed by implementing the process conditions optimized through both the PSO and GA-based methods in the Aspen model and computing the absolute error. Table 14 is dedicated to comparing the execution of PSO and GA models. The results in Table 14 affirm that GA holds a slight advantage over PSO. To illustrate, in data sample 1, GA displays an absolute error of 1.12% whereas PSO records an absolute error of 1.54%. Similarly, in data sample 2, GA exhibits an absolute error of -0.38% while PSO has an absolute error of -0.51%.

**Table 11:** GA and PSO performance validation of heat exchanger network

SR No.	GA exergy efficiency (%)	Aspen model validated exergy efficiency (%)	Absolute error (%)	PSO exergy efficiency (%)	Aspen model validated exergy efficiency (%)	Absolute error (%)
Data Sample 1	73.77	74.61	1.12	73.71	74.86	1.54
Data Sample 2	71.75	71.48	-0.38	71.87	71.50	-0.51
Data Sample 3	68.98	68.61	-0.54	73.12	72.68	-0.61
Data Sample 4	68.55	68.44	-0.16	70.19	69.15	-1.51
Data Sample 5	69.92	69.64	-0.40	69.14	68.70	-0.64
Data Sample 6	69.45	69.27	-0.27	68.67	68.65	-0.03

Data Sample 7	73.00	72.65	-0.48	72.30	72.07	-0.32
Data Sample 8	70.18	69.93	-0.36	69.93	69.65	-0.40
Data Sample 9	72.29	72.06	-0.31	69.54	69.36	-0.26
Data Sample 10	70.69	70.50	-0.27	70.81	70.61	-0.28

## Conclusion

In this study, we employed together traditional and advanced exergy analysis alongside ANN models to assess and optimize the preheat system of a crude oil distillation unit, considering uncertainties. The study aims to achieve the following objectives: to evaluate the system's improvement potential, identify critical areas, and optimize the system while accounting for uncertainties. The overall exergy destruction in HEN is 5403.166 KW, while the exergy efficiency is 66.16%. Furthermore, avoidable exergy destruction is found to be 1759.80 KW, and unavoidable exergy destruction is 3643.35 KW. The seven heat exchangers with the highest exergy destruction rates are identified as priority equipment for intervention because of their substantial influence on the system. Taking steps to reduce avoidable destruction in all the exchangers within the preheat train leads to a substantial decrease of about 1759.80 KW in exergy destruction. This reduction leads to a higher inlet temperature at the furnace, subsequently lowering fuel consumption and environmental impacts.

After conventional and advanced exergy analyses, we developed ANN models and employed them as substitute in PSO and GA frameworks to optimize exergy efficiency beneath uncertain conditions, with a focus on improving exergy efficiency. Our proposed framework surpassed the SA in achieving the superior exergy efficiency. We cross-validated the operation of both PSO and GA by applying the improved specifications to the Aspen model and assessing the absolute error. In conclusion, we found that the working of both PSO and GA exhibited similar results. The integration of ANN models for comprehensive system evaluation, encompassing both exergy and advanced exergy analysis perspectives, along with utilization of GA and PSO frameworks for optimization, not only results in time savings but also conserves valuable computational resources. This study serves as a foundational step toward simulating Refinery 4.0, offering invaluable insights that will undoubtedly guide future initiatives aimed at optimizing energy usage and enhancing overall efficiency.



## Reference

- [1] S. de Oliveira Junior, S. J. E. P. de Oliveira, Cost, and Renewability, "Exergy, exergy costing, and renewability analysis of energy conversion processes," pp. 5-53, 2013.
- [2] A. Al-Ghandoor, P. Phelan, R. Villalobos, and J. J. E. Jaber, "Energy and exergy utilizations of the US manufacturing sector," vol. 35, no. 7, pp. 3048-3065, 2010.
- [3] H. H. Haldorsen and P. J. J. o. P. T. Leach, "Energy 360: Invited perspective: The outlook for energy: A view to 2040," vol. 67, no. 04, pp. 14-19, 2015.
- [4] H. Li, R. Sun, K. Dong, R. J. J. o. C. Guo, and T. Nanoscience, "Refining operations: energy consumption and emission," vol. 13, no. 2, pp. 1497-1502, 2016.
- [5] Y. Han, H. Wu, Z. Geng, Q. Zhu, X. Gu, and B. J. E. Yu, "Energy efficiency evaluation of complex petrochemical industries," vol. 203, p. 117893, 2020.
- [6] S. Macchietto, F. Coletti, and E. D. Bejarano, "Energy recovery in heat exchanger networks in a dynamic, big-data world: design, monitoring, diagnosis and operation," in *Computer Aided Chemical Engineering*, vol. 44: Elsevier, 2018, pp. 1147-1152.
- [7] F. Coletti and S. Macchietto, "Predicting refinery energy losses due to fouling in heat exchangers," in *Computer Aided Chemical Engineering*, vol. 27: Elsevier, 2009, pp. 219-224.
- [8] F. Coletti, S. Macchietto, G. T. J. C. Polley, and c. engineering, "Effects of fouling on performance of retrofitted heat exchanger networks: A thermo-hydraulic based analysis," vol. 35, no. 5, pp. 907-917, 2011.
- [9] F. Coletti, S. Macchietto, and G. T. Polley, "Effects of fouling on performance of retrofitted heat exchanger networks; a thermo-hydraulic based analysis," in *Computer Aided Chemical Engineering*, vol. 28: Elsevier, 2010, pp. 19-24.
- [10] A. Ghannadzadeh and M. J. J. o. C. P. Sadeqzadeh, "Exergy analysis as a scoping tool for cleaner production of chemicals: a case study of an ethylene production process," vol. 129, pp. 508-520, 2016.
- [11] T. Morosuk, G. Tsatsaronis, C. J. E. C. Zhang, and Management, "Conventional thermodynamic and advanced exergetic analysis of a refrigeration machine using a Voorhees' compression process," vol. 60, pp. 143-151, 2012.
- [12] G. J. I. J. o. E. Tsatsaronis, "Recent developments in exergy analysis and exergoeconomics," vol. 5, no. 5-6, pp. 489-499, 2008.

- [13] B. Yuan, Y. Zhang, W. Du, M. Wang, and F. J. A. E. Qian, "Assessment of energy saving potential of an industrial ethylene cracking furnace using advanced exergy analysis," vol. 254, p. 113583, 2019.
- [14] F. Bühler, T.-V. Nguyen, J. K. Jensen, F. M. Holm, and B. J. E. Elmegaard, "Energy, exergy and advanced exergy analysis of a milk processing factory," vol. 162, pp. 576-592, 2018.
- [15] S. Fellaou and T. J. E. Bounahmidi, "Analyzing thermodynamic improvement potential of a selected cement manufacturing process: Advanced exergy analysis," vol. 154, pp. 190-200, 2018.
- [16] R. Mu, M. Liu, and J. J. F. P. T. Yan, "Advanced exergy analysis on supercritical water gasification of coal compared with conventional O<sub>2</sub>-H<sub>2</sub>O and chemical looping coal gasification," vol. 245, p. 107742, 2023.
- [17] M. Mehdizadeh-Fard, F. Pourfayaz, M. Mehrpooya, and A. J. A. T. E. Kasaeian, "Improving energy efficiency in a complex natural gas refinery using combined pinch and advanced exergy analyses," vol. 137, pp. 341-355, 2018.
- [18] B.-H. Li, Y. E. C. Castillo, C.-T. J. C. E. R. Chang, and Design, "An improved design method for retrofitting industrial heat exchanger networks based on Pinch Analysis," vol. 148, pp. 260-270, 2019.
- [19] C. Liang and X. J. C. E. T. Feng, "Heat integration of a continuous reforming process," vol. 25, pp. 213-218, 2011.
- [20] L. M. Ulyev, P. O. Kapustenko, and D. D. Nechiporenko, "The Choice of the Optimal Retrofit Method for Sections of the Catalytic Reforming Unit," 2014.
- [21] I. H. Alhajri, M. A. Gadalla, O. Y. Abdelaziz, and F. H. J. C. S. i. T. E. Ashour, "Retrofit of heat exchanger networks by graphical Pinch Analysis—A case study of a crude oil refinery in Kuwait," vol. 26, p. 101030, 2021.
- [22] M. A. J. E. Gadalla, "A new graphical method for Pinch Analysis applications: Heat exchanger network retrofit and energy integration," vol. 81, pp. 159-174, 2015.
- [23] S. Mrayed, M. B. Shams, M. Al-Khayyat, N. J. C. E. Alnoaimi, and Technology, "Application of pinch analysis to improve the heat integration efficiency in a crude distillation unit," vol. 4, p. 100168, 2021.
- [24] B. S. Babaqi, M. S. Takriff, N. T. A. Othman, and S. K. J. E. Kamarudin, "Yield and energy optimization of the continuous catalytic regeneration reforming process based particle swarm optimization," vol. 206, p. 118098, 2020.

- [25] C. Yan, L. Lv, A. Eslamimanesh, and W. J. A. T. E. Shen, "Application of retrofitted design and optimization framework based on the exergy analysis to a crude oil distillation plant," vol. 154, pp. 637-649, 2019.
- [26] M. Mehdizadeh-Fard, F. Pourfayaz, and A. J. E. R. Maleki, "Exergy analysis of multiple heat exchanger networks: An approach based on the irreversibility distribution ratio," vol. 7, pp. 174-193, 2021.
- [27] Y.-j. Zhao *et al.*, "Pinch combined with exergy analysis for heat exchange network and techno-economic evaluation of coal chemical looping combustion power plant with CO<sub>2</sub> capture," vol. 238, p. 121720, 2022.
- [28] M. Mehdizadeh-Fard and F. J. J. o. C. P. Pourfayaz, "Advanced exergy analysis of heat exchanger network in a complex natural gas refinery," vol. 206, pp. 670-687, 2019.
- [29] J. Fajardo, C. Negrette, D. Yabrudy, and C. Cardona, "Advanced exergetic analysis of preheat train of a crude oil distillation unit," in *ASME International Mechanical Engineering Congress and Exposition*, 2021, vol. 85642, p. V08BT08A007: American Society of Mechanical Engineers.
- [30] A. Kumar, R. Shankar, and L. S. J. J. o. c. s. Thakur, "A big data driven sustainable manufacturing framework for condition-based maintenance prediction," vol. 27, pp. 428-439, 2018.
- [31] I. Ahmad, H. Mabuchi, M. Kano, S. Hasebe, Y. Inoue, and H. J. I. P. V. Uegaki, "Data-based fault diagnosis of power cable system: comparative study of k-NN, ANN, random forest, and CART," vol. 44, no. 1, pp. 12880-12885, 2011.
- [32] I. Ahmad, A. Ayub, U. Ibrahim, M. K. Khattak, and M. J. E. Kano, "Data-based sensing and stochastic analysis of biodiesel production process," vol. 12, no. 1, p. 63, 2018.
- [33] H. Ullah *et al.*, "Optimization based comparative study of machine learning methods for the prediction of bio-oil produced from microalgae via pyrolysis," vol. 170, p. 105879, 2023.
- [34] C. J. J. o. C. P. Camposeco-Negrete, "Optimization of cutting parameters for minimizing energy consumption in turning of AISI 6061 T6 using Taguchi methodology and ANOVA," vol. 53, pp. 195-203, 2013.
- [35] I. Ahmad, M. Kano, S. Hasebe, H. Kitada, and N. J. J. o. C. E. o. J. Murata, "Prediction of molten steel temperature in steel making process with uncertainty by integrating gray-box model and bootstrap filter," vol. 47, no. 11, pp. 827-834, 2014.

- [36] J. Shahzad and I. Ahmad, "Estimation of cutpoint temperature under uncertain feed composition and process conditions using artificial intelligence methods," in *Computer Aided Chemical Engineering*, vol. 50: Elsevier, 2021, pp. 971-976.
- [37] I. Ahmad, M. Kano, S. Hasebe, H. Kitada, and N. J. J. o. P. C. Murata, "Gray-box modeling for prediction and control of molten steel temperature in tundish," vol. 24, no. 4, pp. 375-382, 2014.
- [38] O. Özkaraca, A. Keçebaş, and C. J. E. Demircan, "Comparative thermodynamic evaluation of a geothermal power plant by using the advanced exergy and artificial bee colony methods," vol. 156, pp. 169-180, 2018.
- [39] F. A. Boyaghchi and H. J. E. Molaie, "Advanced exergy and environmental analyses and multi objective optimization of a real combined cycle power plant with supplementary firing using evolutionary algorithm," vol. 93, pp. 2267-2279, 2015.
- [40] L. Liu, R. Zhai, and Y. J. A. E. Hu, "Multi-objective optimization with advanced exergy analysis of a wind-solar-hydrogen multi-energy supply system," vol. 348, p. 121512, 2023.
- [41] M. Khan, I. Ahmad, M. Ahsan, M. Kano, and H. J. F. Caliskan, "Prediction of optimum operating conditions of a furnace under uncertainty: An integrated framework of artificial neural network and genetic algorithm," vol. 330, p. 125563, 2022.
- [42] D. Yabrudy Mercado, J. Fajardo Cuadro, B. Sarria López, C. J. F. i. H. Cardona Agudelo, and M. Transfer, "Efficiency centered maintenance for preheat trains of crude oil distillation units," vol. 15, no. 1, 2020.
- [43] G. T. Polley, D. Wilson, B. Yeap, and S. J. A. T. E. Pugh, "Evaluation of laboratory crude oil threshold fouling data for application to refinery pre-heat trains," vol. 22, no. 7, pp. 777-788, 2002.
- [44] J. H. Gary, J. H. Handwerk, M. J. Kaiser, and D. Geddes, *Petroleum refining: technology and economics*. CRC press, 2007.
- [45] N. Araya, J. Madariaga, and M. J. I. J. o. H. E. Toledo, "Numerical modelling of a three-zone combustion for heavy fuel oil in inert porous media reactor," vol. 46, no. 43, pp. 22385-22396, 2021.
- [46] K. Thulukkanam, *Heat exchanger design handbook*. CRC press, 2000.
- [47] J. Szargut, D. R. Morris, and F. R. Steward, *Exergy analysis of thermal, chemical, and metallurgical processes*. Springer, 1988.

- [48] E. Sciubba and G. J. I. J. o. T. Wall, "A brief commented history of exergy from the beginnings to 2004," vol. 10, no. 1, pp. 1-26, 2007.
- [49] A. Bejan, G. Tsatsaronis, and M. J. Moran, *Thermal design and optimization*. John Wiley & Sons, 1995.
- [50] G. Tsatsaronis and T. J. E. Morosuk, "Advanced exergetic analysis of a novel system for generating electricity and vaporizing liquefied natural gas," vol. 35, no. 2, pp. 820-829, 2010.
- [51] T. Morosuk and G. J. E. Tsatsaronis, "Comparative evaluation of LNG-based cogeneration systems using advanced exergetic analysis," vol. 36, no. 6, pp. 3771-3778, 2011.
- [52] T. Morosuk and G. J. I. J. o. T. Tsatsaronis, "Advanced exergy analysis for chemically reacting systems—application to a simple open gas-turbine system," vol. 12, no. 3, pp. 105-111, 2009.
- [53] G. Tsatsaronis, S. O. Kelly, and T. V. Morosuk, "Endogenous and exogenous exergy destruction in thermal systems," in *ASME International Mechanical Engineering Congress and Exposition*, 2006, vol. 47640, pp. 311-317.
- [54] T. Morosuk and G. Tsatsaronis, "How to calculate the parts of exergy destruction in an advanced exergetic analysis," in *Proceedings of the 21st International Conference on Efficiency, Costs, Optimization, Simulation and Environmental Impact of Energy Systems*, 2008, pp. 185-194: Cracow, Gliwice, Poland, June.
- [55] F. Petrakopoulou, "Comparative evaluation of power plants with CO<sub>2</sub> capture: thermodynamic, economic and environmental performance," 2011.
- [56] S. Kelly, G. Tsatsaronis, and T. J. E. Morosuk, "Advanced exergetic analysis: Approaches for splitting the exergy destruction into endogenous and exogenous parts," vol. 34, no. 3, pp. 384-391, 2009.
- [57] A. Vatani, M. Mehrpooya, A. J. E. c. Palizdar, and management, "Advanced exergetic analysis of five natural gas liquefaction processes," vol. 78, pp. 720-737, 2014.
- [58] G. Tsatsaronis, M.-H. J. E. c. Park, and management, "On avoidable and unavoidable exergy destructions and investment costs in thermal systems," vol. 43, no. 9-12, pp. 1259-1270, 2002.
- [59] J. Yazdanfar, M. Mehrpooya, H. Yousefi, A. J. E. c. Palizdar, and management, "Energy and exergy analysis and optimal design of the hybrid molten carbonate fuel cell power plant and carbon dioxide capturing process," vol. 98, pp. 15-27, 2015.

- [60] A. Al-Shathr, Z. M. Shakor, H. S. Majdi, A. A. AbdulRazak, and T. M. J. C. Albayati, "Comparison between artificial neural network and rigorous mathematical model in simulation of industrial heavy naphtha reforming process," vol. 11, no. 9, p. 1034, 2021.
- [61] T. Gueddar and V. J. A. e. Dua, "Novel model reduction techniques for refinery-wide energy optimisation," vol. 89, no. 1, pp. 117-126, 2012.
- [62] Z. U. Haq, H. Ullah, M. N. A. Khan, S. R. Naqvi, M. J. C. E. R. Ahsan, and Design, "Hydrogen production optimization from sewage sludge supercritical gasification process using machine learning methods integrated with genetic algorithm," vol. 184, pp. 614-626, 2022.
- [63] H. P. J. D. o. c. Gavin and D. U. environmental engineering, "The Levenberg-Marquardt algorithm for nonlinear least squares curve-fitting problems," vol. 19, 2019.
- [64] Z. J. G. S. G. S. D. L. D. L. Michalewicz, "Genetic Algorithms+ Data Structures= Evolution Programs. Springer-Verlag, 1999," 1999.
- [65] S. Katoch, S. S. Chauhan, V. J. M. t. Kumar, and applications, "A review on genetic algorithm: past, present, and future," vol. 80, pp. 8091-8126, 2021.
- [66] G. Cerniauskas and P. J. E. M. L. Alam, "Compressive properties of parametrically optimised mechanical metamaterials based on 3D projections of 4D geometries," vol. 61, p. 102019, 2023.
- [67] M. Kumar, D. M. Husain, N. Upreti, and D. J. A. a. S. Gupta, "Genetic algorithm: Review and application," 2010.
- [68] K. Jebari and M. J. I. J. o. E. S. Madiafi, "Selection methods for genetic algorithms," vol. 3, no. 4, pp. 333-344, 2013.
- [69] G. K. Soon, T. T. Guan, C. K. On, R. Alfred, and P. Anthony, "A comparison on the performance of crossover techniques in video game," in *2013 IEEE international conference on control system, computing and engineering*, 2013, pp. 493-498: IEEE.
- [70] P. Duchêne, L. Mencarelli, A. J. C. Pagot, and C. Engineering, "Optimization approaches to the integrated system of catalytic reforming and isomerization processes in petroleum refinery," vol. 141, p. 107009, 2020.